Utrecht University

Bachelor thesis

Quantum fluctuations and phase transitions in antiferromagnetic spin configurations

Author:
D.T.E. van de Heisteeg
Study:
Physics and Astronomy

Supervisor:
Prof. dr. R.A. Duine
Institute for Theoretical Physics

Utrecht, June 15, 2016.

Abstract

In this thesis we consider quantum fluctuations in the ground state energy of antiferromagnetic spin configurations, and phase transitions between these configurations. We use a Holstein-Primakoff transformation up to second order to transform our spin operators, and a Bogoliubov transformation to diagonalize the corresponding Hamiltonian. First we consider a Hamiltonian with Heisenberg-exchange interaction, a magnetic field and anisotropy, for which we investigated both the the antiferromagnetic phase and the spin-flop phase. For the antiferromagnetic phase we find that quantum fluctuations lower the ground state energy. For the spin-flop phase we find that quantum fluctuations lower the ground state energy even more, such that the phase transition point between these phases is shifted to a slightly lower strength of the magnetic field. Furthermore, this shifted phase transition is caused by ground state energies of the spin-flop phase that become complex, instead of an energy crossing. This energy takes on complex values due to imaginary eigenvalues for magnons, which correspond to exponentially increasing semi-classical spin waves.

Next we considered the Dzyaloshinskii-Moriya interaction (DMI) in one dimension, with the spiral phase it induces. We focused on the magnetic frustration of this phase due to anisotropy and the magnetic field. We used a superposition of two plane waves to describe the deviation due to this frustration, and minimized the ground state energy for their amplitudes numerically. By assuming only spirals of integer length and periodic boundary conditions, we constructed a semi-classical ground state phase diagram between the three mentioned phases. This phase diagram suggests a triple point between these phases when the DMI is zero, at the semi-classical phase transition point between the spin-flop phase and antiferromagnetic phase.

Contents

Chapter 1

Introduction

The magnetic behaviour of materials is caused by the electrons of their atoms. Each electron has an intrinsic magnetic moment, their so-called spin. When the electron shell of an atom is completely filled, the spins of these electrons cancel each other out, and the net magnetic moment of the atom is zero. However, when the outer shell of an atom is only partially filled, these electrons will give the atom a magnetic moment, and the material becomes magnetic. This means that we can often interprete a magnetic material as a lattice of spins, where each spin points in a certain direction. A simple example is the ferromagnetic configuration, where all spins point in the same direction.

In this thesis we will focus on several antiferromagnetic configurations. For a regular antiferromagnet, the lattice consists of alternating spins, i.e. neighbouring spins pointing in opposite directions, such as "up down up down" for a one-dimensional line. Taking different interactions into account, such as a magnetic field, changes this configuration, since spins favour aligning partly along this field. This could cause a spin-flop configuration, which we will investigate in Chapter 4.

All these phases discussed so far are ground states, the states of the magnets at temperature $T = 0$. Increasing the temperature leads to excitations of these ground states. Suppose we have the ground state of a ferromagnet. The simplest excitation is turning one spin in the other direction. This is a common approach in the Ising model, but leads to quite a high energy difference with the ground state, since neighbouring spins favour pointing in the same direction (for ferromagnets). Furthermore, these kind of excitations do not form the eigenstates of the quantum-mechanical Hamiltonian. Due to the wavelike nature of particles in quantum mechanics, spin waves are a much better ansatz for the excitations (see Figure 1.1). Another feature of spin waves is that they require a much lower increase in energy, since the deviation between neighbouring spins is much smaller. It turns out that this approach leads to quantized spin waves called magnons. These are quasiparticles corresponding with the collective excitation of the spins, first introduced by Bloch [1930], and they form the eigenstates of our Hamiltonian.

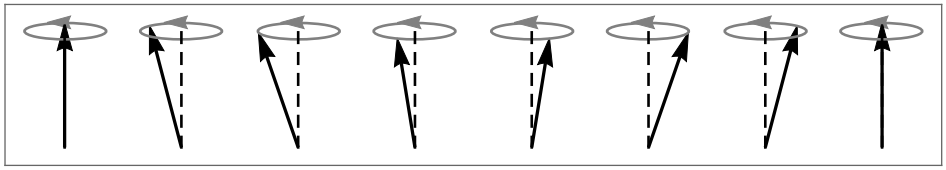

Figure 1.1 – Semi-classical picture of a spin wave going through a one-dimensional ferromagnet, where the spins rotate around their original alignment.

Quantum phase transitions differ from classical phase transitions, in that they occur at temperature $T = 0$ instead of at some critical temperature T_c. For quantum phase transitions, we have a different control parameter g instead of the temperature T, such as a magnetic field for instance. Varying this parameter leads to a quantum critical point

(QCP) at some critical value $g = g_c$ (and $T = 0$). Around this critical point quantum fluctuations determine the behaviour of our material, instead of thermal fluctuations. In this thesis, these quantum fluctuations will be induced by treating the Hamiltonian quantum-mechanically instead of semi-classically. When we increase the temperature and approach the classical phase transition, quantum fluctuations decrease in influence and are dominated by thermal fluctuations. This behaviour is summarized in Figure 1.2.

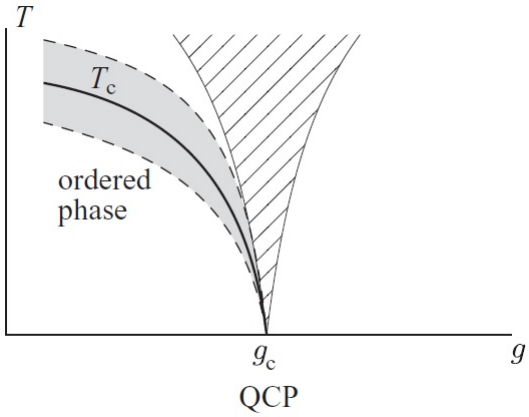

Figure 1.2 – Example of a (quantum) phase diagram, where the domains of both types of fluctuations are specified by the shaded and grey areas. In this diagram the quantum phase transition is coupled to a classical phase transition, but this is not always the case. Without a classical phase transition, the diagram reduces to a line, but quantum fluctuations still exist in the shaded area. Taken directly from Khomskii [2010].

Currently there has been a significant amount of research into quantum phase transitions and fluctuations in magnetic materials, which has lead to the experimental discovery of skyrmions in magnets (Mühlbauer et al. [2009]). They were first introduced as a topological object in particle physics by Skyrme [1962], but this concept turned out to be applicable in many other fields of physics. In magnets a skyrmion is a vortex- or hedgehog-like pattern of the spins, and it has several possible applications in technology, including a new form of data storage. However, there are still some open problems in this field, such as a clear analytical description for these skyrmions in antiferromagnets.

Organization of this thesis

This thesis is a continuation of the Bachelor thesis of van Velzen [2016], and therefore most chapters will be related to her work. The ultimate goal is to determine the effect of quantum fluctuations on the ground state phase diagram of antiferromagnets with anisotropy and Dzyaloshinskii-Moriya interaction.

For each spin configuration that we will consider, we will first analyze semi-classical spin waves going through these spin lattices. We will find that the frequencies that we derive for these spin waves, will correspond to the eigenvalues of our Hamiltonian, and therefore give us some insight in diagonalizing this Hamiltonian. First, in Chapter 2, we will take a look at ferromagnets as an introduction to our methods, using only the Heisenberg-exchange interaction (coupling between neighbouring spins). Then we will consider antiferromagnets. Besides the Heisenberg-exchange interaction, we will incorporate a magnetic field and anisotropy in our Hamiltonian. This gives rise to two configurations, the antiferromagnetic phase (Chapter 3) and the spin-flop phase (Chapter 4). We will analyze the phase transition between these states, and determine whether quantum fluctuations shift this point. In Chapter 5 we will investigate the Dzyaloshinskii-Moriya interaction. Without anisotropy and a magnetic field, this causes a spiral phase, but when we do incorporate these interactions, we get a distortion to this spiral pattern, which we will try to describe through a linearization.

Chapter 2

Ferromagnets

In this chapter we will discuss a regular ferromagnet. To do this, we will analyze the Heisenberg-exchange Hamiltonian, and we will not assume any further interactions between the spins. This interaction causes either ferromagnetic or antiferromagnetic ordering, determined by the sign of the coupling constant J. For a ferromagnet we have $J > 0$, and this Hamiltonian is given by:

$$H = -\frac{J}{2}\sum_i \sum_\delta \mathbf{S}_i \cdot \mathbf{S}_{i+\delta}, \tag{2.0.1}$$

where the sum over i is a sum over all lattice sites, and the sum over δ denotes a sum over all nearest neighbours. Note that we count each pair twice, and that we corrected for this double counting. Furthermore, we will consider a hypercubic lattice in this thesis (with lattice spacing a), i.e. a line as our one-dimensional lattice, and a square or cubic lattice as our two- and three-dimensional lattices respectively. Thus, a site i will correspond with some vector $\mathbf{r}_i$ in the higher-dimensional cases. Furthermore, our δ represents the vectors $\pm a\hat{x}, \pm a\hat{y}, \pm a\hat{z}$ for the three-dimensional lattice, and similar sets for lower-dimensional lattices.

In the first paragraph we will treat the Hamiltonian semi-classically. This means that we interprete each $\mathbf{S}_i$ as a vector that points in the direction of our spin at site i. This direction should minimize the energy of our system. Then we can deduce equations of motion to describe our spin waves, and solve these.
In the second paragraph we will analyze the Hamiltonian quantum-mechanically. This means that we treat each $\mathbf{S}_i$ as an operator. Now we can apply a Holstein-Primakoff transformation to bosonic operators, and deduce a quantum-mechanical ground state energy for our system. We can compare this energy to our semi-classical results.

2.1 Spin waves in the ferromagnetic configuration

In a regular ferromagnetic phase, all spins points in the same direction. We assume that our spins are placed on the $\hat{x}$-axis, and that all spins point in the $\hat{z}$-direction. Note that this does minimize our classical energy (i.e., this is the ground state of our system).[1] The corresponding classical energy is $-J\hbar S$ per spin, where $\hbar S$ is the magnitude of our spins.

Now we want to find the equations of motion for our spin. From Ehrenfest's theorem, we can derive the following equation for the motion of a spin $\mathbf{S}_j$:

$$\frac{\partial \mathbf{S}_j}{\partial t} = -\mathbf{S}_j \times \frac{\partial H}{\partial \mathbf{S}_j}. \tag{2.1.1}$$

[1] Actually, we could have chosen any direction, not only the $\hat{z}$-direction, as long as all spins point in the same direction.

The partial derivative on the right-hand side is given by $-J(\mathbf{S}_{j-1} + \mathbf{S}_{j+1})$. There is one problem however. First we assumed that all spins were static and point in the same direction. In this case we would find that the time derivative on the left-hand side vanishes, just as the cross product on the right-hand side vanishes. For a spin wave through the lattice, this is obviously not the case. Therefore, we will assume that our spins have small deviations perpendicular to the original direction of the spin, that do depend on the time and site $(\delta S_j^x, \delta S_j^y)$. Mathematically we can express this in the following formula:

$$\mathbf{S}_j = \delta S_j^x \hat{x} + \delta S_j^y \hat{y} + \hbar S \hat{z}, \tag{2.1.2}$$

where $\hbar S$ is the original magnitude of our spin. Applying this formula to Equation 2.1.1, we get the following equations of motion:

$$\begin{aligned} \delta \dot{S}_j^x &= 2J\hbar S \delta S_j^y - J\hbar S\big(\delta S_{j-1}^y + \delta S_{j+1}^y\big), \\ \delta \dot{S}_j^y &= J\hbar S\big(\delta S_{j-1}^x + \delta S_{j+1}^x\big) - 2J\hbar S \delta S_j^x, \end{aligned} \tag{2.1.3}$$

where the equation for the $\hat{z}$-component vanishes, since both sides are equal to zero.[2] Now we need to make some kind of ansatz to solve these equations. We expect a spin wave through our lattice, so we make the following plane-wave ansatz:

$$\begin{aligned} \delta S_j^x &= A_x e^{i(kja - \omega t)}, \\ \delta S_j^y &= A_y e^{i(kja - \omega t)}, \end{aligned} \tag{2.1.4}$$

where k is our wave constant, ω is our frequency, and A_x, A_y are our amplitudes. Filling these formulas in into our equations of motion, we get the following set of equations:

$$\begin{aligned} -i\omega A_x &= 2J\hbar S A_y - 2J\hbar S \cos(ka) A_y, \\ -i\omega A_y &= 2J\hbar S \cos(ka) A_x - 2J\hbar S A_x, \end{aligned} \tag{2.1.5}$$

where we divided both equations by our exponential $\exp[i(kja - \omega t)]$ to derive these relations between the amplitudes. We can put this set of equations into the following matrix equation:

$$\begin{pmatrix} i\omega & 2J\hbar S - 2J\hbar S\cos(ka) \\ 2J\hbar S\cos(ka) - 2J\hbar S & i\omega \end{pmatrix} \begin{pmatrix} A_x \\ A_y \end{pmatrix} = 0. \tag{2.1.6}$$

Now we have a solution for A_x, A_y, provided that the determinant of the matrix is equal to zero. Solving this for ω yields the following dispersion relation:

$$\omega_k = 2J\hbar S\big(1 - \cos(ka)\big). \tag{2.1.7}$$

This dispersion relation has been depicted graphically in Figure 2.1. From this dispersion relation we can derive the following eigenvector (for all values of k):

$$v = \begin{pmatrix} i \\ 1 \end{pmatrix}. \tag{2.1.8}$$

The other eigenvector gives us the static solution, i.e. $A_x = A_y = 0$.
We can combine the non-zero eigenvector with our plane-wave ansatz to find the following (real) solution:

$$\begin{aligned} \delta S_j^x &\propto -\sin(kja - \omega_k t), \\ \delta S_j^y &\propto \cos(kja - \omega_k t). \end{aligned} \tag{2.1.9}$$

This spin wave can be interpreted as a precessing spin at each site. The term kja stands for a phase shift, where each next spin is rotated by ka with respect to the previous spin. Furthermore, we find at $k = 0$ that our frequency is also zero. This means that

[2] Note that the left-hand side is zero, because our spins are constant in the $\hat{z}$-direction and we take a time derivative, while the right hand side is zero because it is second order in our small deviations, and we can neglect these terms.

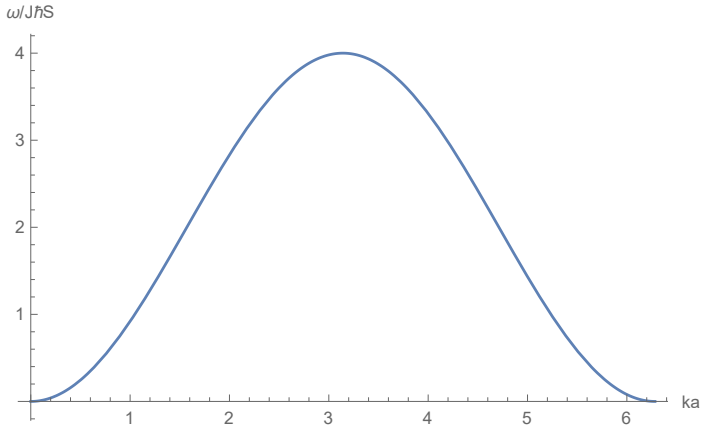

Figure 2.1 – Dispersion relation for spin waves throught a one-dimensional ferromagnetic lattice.

our spins are rotated to another (static) direction, which is the same direction for all spins. Physically, this can be explained by a symmetry for our spin configuration. As mentioned earlier, we could have chosen any direction for the spins to point to, not only the $\hat{z}$-direction, as long as all spins point in the same direction. This spin wave just corresponds to (the spontaneous breaking of) this symmetry. Modes like this are commonly called Goldstone modes, and were first hypothesized by Goldstone et al. [1962].

A typical feature of Goldstone modes is that they do not cost any energy at $k = 0$. For our semi-classical spin waves, this can be explained by the symmetry between the two configuration with and without the spin wave. This argument would be a bit different from a quantum-mechanical point of view. Then we would treat these spin waves as quasiparticles called magnons, each with an energy $\hbar\omega_k$. Since the frequency is zero at $k = 0$, we find that our magnons are gapless, and thus that they obey Goldstone's theorem. Furthermore, we will find this suggested relation between semi-classical spin waves and magnons in the next paragraph. The frequencies of these spin waves will correspond with the eigenvalues and eigenstates of our Hamiltonian, which are these magnons. For the semi-classical analysis we can conclude that spin waves are not included in the ground state, since they increase the energy of our system for $k \neq 0$.

2.2 Quantum-mechanical approach

Now we will treat our Hamiltonian as a quantum-mechanical operator. We will need to use a Holstein-Primakoff transformation to transform our spin operators (Holstein and Primakoff [1940]). This is a mapping from the angular momentum operators to bosonic creation and annihilation operators. Here, the S_i^z-component must be aligned along the (classical) direction of the spin at site i. This is always the $\hat{z}$-direction for our ferromagnet, hence the superscript z. For other spin configurations, we should be more careful with this. This transformation is given by:

$$\begin{aligned} S_i^+ &= \hbar\sqrt{2S - a_i^\dagger a_i}\, a_i \simeq \sqrt{2S}\hbar a_i, \\ S_i^- &= \hbar a_i^\dagger \sqrt{2S - a_i^\dagger a_i} \simeq \sqrt{2S}\hbar a_i^\dagger, \\ S_i^z &= \hbar S - a_i^\dagger a_i, \end{aligned} \tag{2.2.1}$$

where we used a Taylor expansion in $1/S$ to derive our final expressions. We neglect any higher orders in $1/S$, since we assume that S is large and because we are only interested in the ground state energy, not magnon-magnon interactions. Furthermore, $a_i^\dagger$ and a_i are the boson creation and annihilation operators, and these obey the bosonic commutation relation $[a_i, a_j^\dagger] = \delta_{ij}$ (and $[a_i, a_j] = [a_i^\dagger, a_j^\dagger] = 0$). Together, as the operator $n_i = a_i^\dagger a_i$,

they count the boson number at site i. Because of this, we need that $\langle n_i \rangle \leq 2S$, since otherwise our final expressions do not seperate the non-physical states from the physical ones. Suppose for instance that $\langle n_i \rangle > 2S$. Then the expected values for our initial spin raising and lowering operators, $\langle S_i^{\pm} \rangle$, would become imaginary. This is not the case for our expressions after the Taylor expansion, hence the remark.

Furthermore, we need to express our spin raising and lowering operators $S_i^{\pm}$ in terms of the components of our spin. We know that we have the relation $S_i^{\pm} = S_i^x \pm i S_i^y$ for these operators. Using this, we can rewrite the Hamiltonian as the following expression:

$$H = -\frac{J}{2} \sum_i \sum_\delta \left(S_i^z S_{i+\delta}^z + \frac{1}{2} S_i^+ S_{i+\delta}^- + \frac{1}{2} S_i^- S_{i+\delta}^+ \right). \tag{2.2.2}$$

Consider these last two terms, $S_i^+ S_{i+\delta}^-$ and $S_i^- S_{i+\delta}^+$. The first term raises the spin at site i, while it lowers the neighbouring spins, whereas the second term does exactly the opposite. This makes it seem as if there is some kind of spin wave going through our lattice for an eigenstate of this Hamiltonian. We can take a further look at this by applying our Holstein-Primakoff transformation from Equation 2.2.1. When we write out the products in our Hamiltonian, we only include terms up to order two in our bosonic operators, for similar reasons as the Taylor expansion of our Holstein-Primakoff transformation. This gives us the following Hamiltonian:

$$H = -\frac{J}{2} \hbar^2 S \sum_i \sum_\delta \left(S - a_i^\dagger a_i - a_{i+\delta}^\dagger a_{i+\delta} + a_{i+\delta}^\dagger a_i + a_i^\dagger a_{i+\delta} \right). \tag{2.2.3}$$

This Hamiltonian is not diagonal, and we need a diagonalized Hamiltonian to be able to describe the ground state energy and eigenstates. To do this, we apply a Fourier transformation on our bosonic operators:

$$a_i = \frac{1}{\sqrt{N}} \sum_{\mathbf{k}} e^{i\mathbf{k}\cdot\mathbf{r}_i} a_{\mathbf{k}}, \tag{2.2.4}$$

where we introduced a wave vector $\mathbf{k}$ as part of our Fourier transformation, and obviously $a_i^\dagger$ is given by the hermitian conjugate of this expression. Note that it is important that every transformation of these operators preserves the bosonic commutation relations, which is indeed the case for this Fourier transformation.

Now we want to apply this transformation on our Hamiltonian. There are some general identities involving this Fourier transformation included in Appendix A.3, to simplify the expressions. Using these, we can rewrite our Hamiltonian as:

$$H = -\frac{z}{2} J \hbar^2 S^2 N + z J \hbar^2 S \sum_{\mathbf{k}} a_{\mathbf{k}}^\dagger a_{\mathbf{k}} \big(1 - \gamma_{\mathbf{k}}\big), \tag{2.2.5}$$

where we defined $z\gamma_{\mathbf{k}} = \sum_\delta \cos(\mathbf{k} \cdot \delta)$, with z the number of nearest neighbours and N the number of lattice sites. Now we can define $E_0 = -zJ\hbar^2 S^2 N/2$ and $\omega_{\mathbf{k}} = zJ\hbar S\big(1 - \gamma_{\mathbf{k}}\big)$, which simplifies our expression as:

$$H = E_0 + \sum_{\mathbf{k}} \hbar \omega_{\mathbf{k}} a_{\mathbf{k}}^\dagger a_{\mathbf{k}}. \tag{2.2.6}$$

Note that our frequency reduces to $\omega_{\mathbf{k}} = 2J\hbar S\big(1 - \cos(k_x a)\big)$ in the one-dimensional case, which is the same frequency as for our semi-classical spin wave. Thus we find indeed that there is a correspondence between the frequency of semi-classical spin waves and the eigenvalues of our Hamiltonian. Furthermore, this Hamiltonian is now given by a sum over independent harmonic oscillators, each corresponding with a wave vector $\mathbf{k}$. The quanta of these harmonic oscillators are the earlier mentioned magnons, spin waves, and they form the eigenstates of this Hamiltonian. Similar to our semi-classical results, we see that these magnons have a positive energy $\hbar\omega_{\mathbf{k}} > 0$. Thus there are no magnons included in the ground state. Furthermore, we find the same ground state energy as in our semi-classical approach, and we can conclude that quantum fluctuations do not shift this energy for ferromagnets.

Chapter 3

Antiferromagnet in a magnetic field

Now we will consider a regular antiferromagnet. To make our system more realistic, we will take a few other types of interactions into consideration. Besides the Heisenberg-exchange interaction with $J < 0$, we will assume interaction with a magnetic field of strength B, and anisotropy (easy-axis) of strength $K < 0$. Note that we incorporate the strength of the spin with respect to the magnetic field, such as the Bohr magneton μ_B, in the value of B, for convenience in notation. Furthermore, we assume that this magnetic field is applied along the easy axis of the system, which we define as our $\hat{z}$-axis. This means that spins favour the $+\hat{z}$-direction due to the magnetic field, and the $\pm\hat{z}$-directions due to anisotropy. Combining these interactions, we get the following Hamiltonian:

$$H = -\frac{J}{2}\sum_i \sum_\delta \mathbf{S}_i \cdot \mathbf{S}_{i+\delta} - B\sum_i \mathbf{S}_i \cdot \hat{z} + K\sum_i \left(\mathbf{S}_i \cdot \hat{z}\right)^2. \tag{3.0.1}$$

3.1 Spin waves in an antiferromagnetic configuration

The antiferromagnetic state corresponds with a lattice where neighbouring spins are aligned antiparallel, i.e. they point in opposite directions. This means that we have two different directions for our spins. To deal with this, we introduce a local rotated coordinate system, as described in Appendix A.1. We divide our lattice into two sublattices A and B, each corresponding with one of the directions. In such a coordinate system, the third axis will describe the direction of our spin in spherical coordinates (with θ the polar angle and ϕ the azimuthal angle). This means that, if A consists of all spins that point up, and B consists of all spins that point down, we get for sublattice A the angles $\theta_A = \phi_A = 0$, and for sublattice B the angles $\theta_B = \pi$ and $\phi_B = 0$. Then we get the following vectors as the local rotated bases for our sublattices:

$$\begin{aligned} \hat{e}_1^A &= \hat{x}, \quad \hat{e}_1^B = -\hat{x}, \\ \hat{e}_2^A &= \hat{y}, \quad \hat{e}_2^B = \hat{y}, \\ \hat{e}_3^A &= \hat{z}, \quad \hat{e}_3^B = -\hat{z}. \end{aligned} \tag{3.1.1}$$

The classical energy of one spin of this system is given by $E^{AFM} = zJ\hbar^2S^2/2 + K\hbar^2S^2$. Note that the energy due to the magnetic field drops out in this expression, because of the alternating pattern of the antiferromagnetic state. Now we want to describe a spin wave in this lattice. Just like in Chapter 2, we can use the equation from Ehrenfest's theorem to describe the motion of our spin wave. However, the partial derivative of the Hamiltonian will look a bit different, since we have two sublattices instead of one lattice, and two extra interactions. Identifying $\mathbf{S}_j^A$ and $\mathbf{S}_j^B$ with their corresponding sublattices,

we get the following equations of motion:

$$\begin{aligned}\frac{\partial \mathbf{S}_j^A}{\partial t} &= -\mathbf{S}_j^A \times [-J\sum_\delta \mathbf{S}_{j+\delta}^B - B\hat{z} + 2K(\mathbf{S}_j^A \cdot \hat{z})\hat{z}],\\ \frac{\partial \mathbf{S}_j^B}{\partial t} &= -\mathbf{S}_j^B \times [-J\sum_\delta \mathbf{S}_{j+\delta}^A - B\hat{z} + 2K(\mathbf{S}_j^B \cdot \hat{z})\hat{z}].\end{aligned} \tag{3.1.2}$$

Now we can apply similar small deviations as in chapter 2 to our spin vectors, but each in their own local basis:

$$\begin{aligned}\mathbf{S}_j^A &= \delta S_j^{A,1}\hat{e}_1^A + \delta S_j^{A,2}\hat{e}_2^A + \hbar S\hat{e}_3^A,\\ \mathbf{S}_j^B &= \delta S_j^{B,1}\hat{e}_1^B + \delta S_j^{B,2}\hat{e}_2^B + \hbar S\hat{e}_3^B.\end{aligned} \tag{3.1.3}$$

Filling these formulas in into our equations of motion, we get the equations for our small deviations:

$$\begin{aligned}\delta\dot{S}_j^{A,1} &= \big(-zJ\hbar S + B - 2K\hbar S\big)\delta S_j^{A,2} - J\hbar S\sum_\delta \delta S_{j+\delta}^{B,2},\\ \delta\dot{S}_j^{A,2} &= -\big(-zJ\hbar S + B - 2K\hbar S\big)\delta S_j^{A,1} - J\hbar S\sum_\delta \delta S_{j+\delta}^{B,1},\\ \delta\dot{S}_j^{B,1} &= -J\hbar S\sum_\delta \delta S_{j+\delta}^{A,2} - \big(zJ\hbar S + B + 2K\hbar S\big)\delta S_j^{B,2},\\ \delta\dot{S}_j^{B,2} &= -J\hbar S\sum_\delta \delta S_{j+\delta}^{A,1} + \big(zJ\hbar S + B + 2K\hbar S\big)\delta S_j^{B,1},\end{aligned} \tag{3.1.4}$$

where z is the coordination number, i.e. the number of nearest neighbours. Note that, like in the previous chapter, we didn't write down our equations for the third component, since we can neglect terms of order two or higher. Now we can make a wave ansatz for the spins of both sublattices, similar to Chapter 2:

$$\begin{aligned}\delta S_j^{A,i} &= A_i \exp[i(\mathbf{k}\cdot\mathbf{r}_j - \omega t)] \text{ for } i = 1,2,\\ \delta S_j^{B,i} &= B_i \exp[i(\mathbf{k}\cdot\mathbf{r}_j - \omega t)] \text{ for } i = 1,2,\end{aligned} \tag{3.1.5}$$

where A_i, B_i are our amplitudes, $\mathbf{k}$ is our wave vector and ω is our frequency. Filling this ansatz in into our equations of motion, we get the following set of relations between our amplitudes:

$$\begin{aligned}-i\omega A_1 &= \big(-zJ\hbar S + B - 2K\hbar S\big)A_2 - zJ\hbar S\gamma_{\mathbf{k}} B_2,\\ -i\omega A_2 &= -\big(-zJ\hbar S + B - 2K\hbar S\big)A_1 - zJ\hbar S\gamma_{\mathbf{k}} B_1,\\ -i\omega B_1 &= -zJ\hbar S\gamma_{\mathbf{k}} A_2 - \big(zJ\hbar S + B + 2K\hbar S\big)B_2,\\ -i\omega B_2 &= -zJ\hbar S\gamma_{\mathbf{k}} A_1 + \big(zJ\hbar S + B + 2K\hbar S\big)B_1,\end{aligned} \tag{3.1.6}$$

where we defined the phase factor $z\gamma_{\mathbf{k}} = \sum_\delta \cos(\mathbf{k}\cdot\delta)$. Now we can sort these relations between the amplitudes into the following matrix:

$$\begin{pmatrix} i\omega & -zJ\hbar S + B - 2K\hbar S & 0 & -zJ\hbar S\gamma_{\mathbf{k}} \\ zJ\hbar S - B + 2K\hbar S & i\omega & -zJ\hbar S\gamma_{\mathbf{k}} & 0 \\ 0 & -zJ\hbar S\gamma_{\mathbf{k}} & i\omega & -zJ\hbar S - B - 2K\hbar S \\ -zJ\hbar S\gamma_{\mathbf{k}} & 0 & zJ\hbar S + B + 2K\hbar S & i\omega \end{pmatrix}. \tag{3.1.7}$$

We know that we have solutions for our amplitudes when the determinant of this matrix is zero. Solving this determinant equation for ω, we find four solutions for our dispersion relation:

$$\omega_{\mathbf{k}} = \pm B \pm \hbar S\sqrt{4K^2 + 4zJK + z^2J^2(1-\gamma_{\mathbf{k}}^2)}. \tag{3.1.8}$$

For symmetry reasons, we can neglect the negative frequencies of these dispersion relations, since these waves are similar but move in the other direction. Then our one-dimensional dispersion relation reduces to $\omega_{k_x}^{\pm} = |B \pm 2\hbar S\sqrt{(J+K)^2 - J^2\cos^2(k_x a)}|$. These frequencies correspond with the following eigenvectors $u^{\pm}$ at $k_x = 0$:

$$u^{\pm} = \begin{pmatrix} -i\alpha^{\pm} \\ -\alpha^{\pm} \\ -i \\ 1 \end{pmatrix}, \tag{3.1.9}$$

where we have defined the constant $\alpha^{\pm} = 1 + K/J \pm \sqrt{K/J(2+K/J)}$. This means that we get a scaling between the amplitudes of neighbouring spins. This scaling is caused by the anisotropy K, and this scaling is independent of the magnetic field strength B. Furthermore, spins in lattice A rotate clockwise in their $\hat{e}_1^A, \hat{e}_2^A$-plane, while the spins in lattice B rotate counterclockwise in their $\hat{e}_1^B, \hat{e}_2^B$-plane. Also, there is a phase shift between the two sublattices due to different eigenvectors, namely $(-i, -1)$ versus $(-i, 1)$. This means that if $\alpha^{\pm} = 1$, i.e. $K = 0$, then neighbouring spins would be aligned antiparallel during their entire rotation. The anisotropy causes a small deviation from this case. Altogether, the spin waves $v^{\pm}$ will scale as:

$$v^{\pm} \propto \begin{pmatrix} -\alpha^{\pm}\sin\omega_0^{\pm}t \\ -\alpha^{\pm}\cos\omega_0^{\pm}t \\ -\sin\omega_0^{\pm}t \\ \cos\omega_0^{\pm}t \end{pmatrix}. \tag{3.1.10}$$

Furthermore, we find that there is a minimum value for B such that $\omega_{\mathbf{k}}^{-} = 0$ for some value of $\mathbf{k}$, as we can observe in Figure 3.1. Otherwise, they are similar but shifted by $2B$. This point is given by $B = 2\hbar S\sqrt{K(K+zJ)}$, which has the value $B/|J|\hbar S = 0.571314$ in the one-dimensional case, for $K/|J| = -0.04$. In the next paragraph we will find that this point corresponds to magnons with negative eigenvalues.

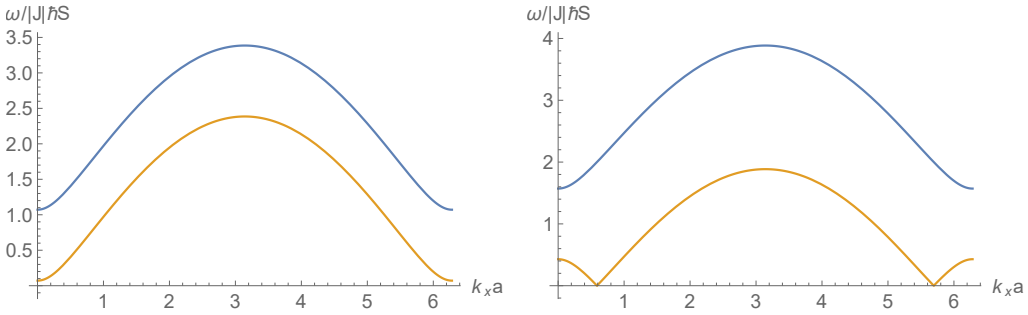

(a) $K/|J| = -0.04$ and $B/|J|\hbar S = 0.5$. **(b)** $K/|J| = -0.04$ and $B/|J|\hbar S = 1$.

Figure 3.1 – Dispersion relations of spin waves for the antiferromagnet for two different values of the magnetic field.

3.2 Quantum-mechanical approach

Now we will treat our Hamiltonian as a quantum-mechanical operator. We assume the same rotated local coordinate systems as in the semi-classical approach, where the Holstein-Primakoff transformation will be applied along $\hat{e}_3^A$ and $\hat{e}_3^B$ (see Appendix A.1 for a more detailed explanation). This will give us two types of bosonic operators, a_i and b_i, corresponding with the sublattices A and B.

Altogether, we can write down the following Hamiltonian:

$$\begin{aligned} H =& H_0 + \frac{1}{2}J\hbar^2 S\left(\sum_{i\in A}\sum_{\delta}\left(a_i b_{i+\delta} + a_i^\dagger b_{i+\delta}^\dagger - 2a_i^\dagger a_i\right) + \sum_{i\in B}\sum_{\delta}\left(b_i a_{i+\delta} + b_i^\dagger a_{i+\delta}^\dagger - 2b_i^\dagger b_i\right)\right) \\ &+ B\hbar\left(\sum_{i\in A} a_i^\dagger a_i - \sum_{i\in B} b_i^\dagger b_i\right) - 2K\hbar^2 S\left(\sum_{i\in A} a_i^\dagger a_i + \sum_{i\in B} b_i^\dagger b_i\right), \end{aligned} \tag{3.2.1}$$

where $H_0 = zJ\hbar^2 S^2 N/2 + K\hbar^2 S^2 N$, with N the number of lattice sites. Then we can apply a Fourier transformation to rewrite this Hamiltonian, according to:

$$\begin{aligned} a_j &= \frac{1}{\sqrt{N_a}}\sum_{\mathbf{k}} e^{i\mathbf{k}\cdot\mathbf{r}_j} a_{\mathbf{k}}, \\ b_j &= \frac{1}{\sqrt{N_b}}\sum_{\mathbf{k}} e^{i\mathbf{k}\cdot\mathbf{r}_j} b_{\mathbf{k}}. \end{aligned} \tag{3.2.2}$$

Using some summation identities for these operators (see Appendix A.3), we get the following Hamiltonian:

$$\begin{aligned} H =& H_0 - (zJ+2K)\hbar^2 S\sum_{\mathbf{k}}\left(a_{\mathbf{k}}^\dagger a_{\mathbf{k}} + b_{\mathbf{k}}^\dagger b_{\mathbf{k}}\right) + B\hbar\sum_{\mathbf{k}}\left(a_{\mathbf{k}}^\dagger a_{\mathbf{k}} - b_{\mathbf{k}}^\dagger b_{\mathbf{k}}\right) \\ &- zJ\hbar^2 S\sum_{k}\gamma_{\mathbf{k}}\left(a_{\mathbf{k}} b_{-\mathbf{k}} + a_{\mathbf{k}}^\dagger b_{-\mathbf{k}}^\dagger\right), \end{aligned} \tag{3.2.3}$$

where again $z\gamma_{\mathbf{k}} = \sum_\delta \cos(\mathbf{k}\cdot\delta)$. Now we are going to write this Hamiltonian in the desired form of Method 2 of Appendix A.2. There we work out a more general form of a Bogoliubov transformation. This is a transformation of bosonic operators that preserves the commutation relations, and can be used to diagonalize our Hamiltonian, developed by Bogoliubov [1958]. By defining $A_{\mathbf{k}} = -(zJ+2K)\hbar^2 S$, $B_{\mathbf{k}} = -zJ\hbar^2 S\gamma_{\mathbf{k}}$ and $C_{\mathbf{k}} = B\hbar$, we get a similar form as this method. This gives us the following Hamiltonian:

$$H = E_0 + \sum_{\mathbf{k}}\hbar\omega_{\mathbf{k}}^+(\alpha_{\mathbf{k}}^\dagger\alpha_{\mathbf{k}} + \frac{1}{2}) + \sum_{\mathbf{k}}\hbar\omega_{\mathbf{k}}^-(\beta_{\mathbf{k}}^\dagger\beta_{\mathbf{k}} + \frac{1}{2}), \tag{3.2.4}$$

where $E_0 = H_0 + (zJ+2K)\hbar^2 SN/2$,[1] and $\omega_{\mathbf{k}}^\pm = \pm B + \hbar S\sqrt{(zJ+2K)^2 - (zJ)^2\gamma_{\mathbf{k}}^2}$. These are the same frequencies as we found in the semi-classical approach. Also, the ground state energy is given by:

$$\begin{aligned} E_{GS} &= E_0 + \frac{1}{2}\sum_{\mathbf{k}}\left(\hbar\omega_{\mathbf{k}}^+ + \hbar\omega_{\mathbf{k}}^-\right) \\ &= \frac{z}{2}J\hbar^2 S^2 N + K\hbar^2 S^2 N + \frac{1}{2}(zJ+2K)\hbar^2 SN + \sum_{\mathbf{k}}\hbar^2 S\sqrt{(zJ+2K)^2 - (zJ)^2\gamma_{\mathbf{k}}^2}. \end{aligned} \tag{3.2.5}$$

Note that this energy is lower than the classical energy, since J and K are negative. Thus we see that quantum fluctuations lower the ground state energy for a regular antiferromagnet.[2] Furthermore, as discussed in the previous paragraph, we find that there are cases where magnons have negative eigenvalues. This means that these magnons could be part of the ground state. The condition is that the strength of the magnetic field must be high enough, namely $B \geq 2\hbar S\sqrt{K(zJ+K)}$. In the next chapter we will find that, for these values of the magnetic field B, antiferromagnets prefer to be in a different configuration. Thus we can still say that we do not expect magnons in the ground state of the regular antiferromagnet, but we will discuss this in more detail in Chapter 6.

[1] Note that we have a factor $N/2$ instead of N. This factor arises because we had a sum over $\mathbf{k}$, but since we have two sublattices instead of one lattice, this gives us $N/2$ terms instead of N terms

[2] Actually, there is also a shift upwards due to the sum over the frequencies, but in general this sum is smaller.

Chapter 4

Spin-flop state and phase transition

In this chapter we will consider the spin-flop phase for antiferromagnets. We will analyze this phase with the same Hamiltonian as the regular antiferromagnet, i.e. with Heisenberg-exchange interaction, a magnetic field and anisotropy. We can deduce what this configuration looks like from the limit $B \gg |J|\hbar S$. In this limit the system favours that all spins point in the direction of the magnetic field, the $\hat{z}$-direction. When we lower the strength of our magnetic field, the negative coupling constant J will increase in influence. This will cause an alternating pattern of the spins in the xy-plane, while their z-component will decrease accordingly. This can be visualized as in Figure 4.1.

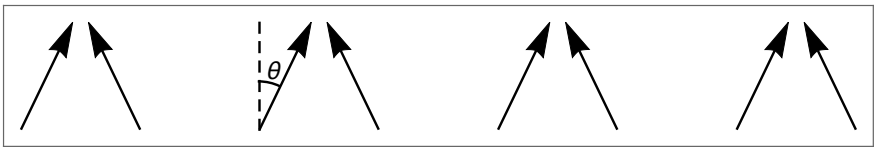

Figure 4.1 – Graphical depiction of the spin-flop state in the xz-plane.

The angle of this flop, θ, must minimize the classical energy of our Hamiltonian. This is the first calculation we will perform. Furthermore, we will compare this energy to the energy of the antiferromagnet, and determine the point of the phase transition for the magnetic field B. Then we will take a look at spin waves through this lattice. In the next paragraph we will treat this state quantum-mechanically, diagonalize the corresponding Hamiltonian and determine the ground state energy. This energy will be compared to the (quantum) ground state energy of the antiferromagnet, and we will determine wether quantum fluctuations shift the phase transition.

4.1 Spin waves and ground state energies

First we are going to minimize the classical energy of one spin to determine the angle of our flop. We can divide our lattice into two sublattices A and B, as we did for the antiferromagnet. Similarly, we will use a local rotated coordinate system to describe the spin vectors of both sublattices (Appendix A.1). As mentioned, we want spins of different sublattices to point in opposite directions in the xy-plane, and to have the same magnitude in the $\hat{z}$-direction. The first condition corresponds with $\phi_i = \pi i$, [1] or, for the sublattices, $\phi_A = 0$ and $\phi_B = \pi$. From minimizing the classical energy we find the angle $\theta = \arccos[B/(2\hbar S(K - zJ))]$.

[1] In fact, this angle could correspond with $\phi_i = \pi i + \phi_0$, where ϕ_0 is an added constant rotation. This rotation is possible because of the rotational symmetry in the xy-plane, as long as two neighbouring spins point in opposite directions in this plane.

Then our local rotated coordinate systems are given by:

$$\begin{aligned} \hat{e}_1^A &= (x, 0, -y), \quad \hat{e}_1^B = (-x, 0, -y), \\ \hat{e}_2^A &= (0, 1, 0), \qquad \hat{e}_2^B = (0, -1, 0), \\ \hat{e}_3^A &= (y, 0, x), \qquad \hat{e}_3^B = (-y, 0, x), \end{aligned} \tag{4.1.1}$$

where $x = B/(2\hbar S(K - zJ))$ and $y = \sqrt{1 - x^2}$. Now we want to compare the classical energy of this spin-flop phase with the energy of the antiferromagnetic phase. These energies (per spin) are given by:

$$\begin{aligned} E^{SF} &= \frac{z}{2} J\hbar^2 S^2 - \frac{B^2}{4(K - zJ)}, \\ E^{AFM} &= \frac{z}{2} J\hbar^2 S^2 + K\hbar^2 S^2. \end{aligned} \tag{4.1.2}$$

Using these expressions, we find that the phase transition occurs at $B = 2\hbar S\sqrt{K(zJ - K)}$. Below this value the system will favour the antiferromagnetic ordering, and above this value the spin-flop ordering. When we analyzed the regular antiferromagnetic ordering, we found that there exist magnons with negative eigenvalues for $B > 2\hbar S\sqrt{K(zJ + K)}$. However, the phase transition point we just found, occurs at a lower value for the magnetic field B. Thus, from a semi-classical point of view, we can already argue that these magnons with negative eigenvalues are not included in any ground state, since the system will form a spin-flop configuration instead of an antiferromagnetic configuration. A shift due to quantum fluctuations in this phase transition point could (but doesn't) change this, as we will find in the next paragraph.

Now we will derive our equations of motion for a spin wave. We will use the same equation of motion that followed from Ehrenfest's theorem as in Chapter 3, but now with the spin vectors of the spin-flop phase, i.e. the $\hat{e}_3^A$- and $\hat{e}_3^B$-directions. Again assuming small deviations in the directions perpendicular to the spin vectors, we get the following equations of motion for these deviations:

$$\begin{aligned} \delta\dot{S}_j^{A,1} &= -zJ\hbar S\delta S_j^{A,2} + J\hbar S\sum_\delta \delta S_{j+\delta}^{B,2}, \\ \delta\dot{S}_j^{A,2} &= (zJ\hbar S - 2K\hbar S y^2)\delta S_j^{A,1} + (1 - 2x^2)J\hbar S\sum_\delta \delta S_{j+\delta}^{B,1}, \\ \delta\dot{S}_j^{B,1} &= J\hbar S\sum_\delta \delta S_{j+\delta}^{A,2} - zJ\hbar S\delta S_j^{B,2}, \\ \delta\dot{S}_j^{B,2} &= (1 - 2x^2)J\hbar S\sum_\delta \delta S_{j+\delta}^{A,1} + (zJ\hbar S - 2K\hbar S y^2)\delta S_j^{B,1}, \end{aligned} \tag{4.1.3}$$

where the equations for the third components vanish as usual. Applying a similar wave ansatz as in the previous chapter, this yields the following set of equations:

$$\begin{aligned} -i\omega A_1 &= -zJ\hbar S A_2 + zJ\hbar S\gamma_{\mathbf{k}} B_2, \\ -i\omega A_2 &= (zJ\hbar S - 2K\hbar S y^2)A_1 + (1 - 2x^2)zJ\hbar S\gamma_{\mathbf{k}} B_1, \\ -i\omega B_1 &= zJ\hbar S\gamma_{\mathbf{k}} A_2 - zJ\hbar S B_2, \\ -i\omega B_2 &= (1 - 2x^2)zJ\hbar S\gamma_{\mathbf{k}} A_1 + (zJ\hbar S - 2K\hbar S y^2)B_1, \end{aligned} \tag{4.1.4}$$

where we used the phase factor $z\gamma_{\mathbf{k}} = \sum_\delta \cos(\mathbf{k} \cdot \delta)$ again. Now we do note a symmetry in these equations between our sublattices A and B. Namely, we can change A_1 with B_1 and A_2 with B_2, and then our equations of motions will stay the same. This symmetry corresponds to rotating by π around the $\hat{z}$-axis, and we could have used this earlier to reduce our system to one lattice. However, it is easier to adjust for this symmetry now, and set $A_1 = B_1$ and $A_2 = B_2$. This gives the following two equations of motions:

$$\begin{aligned} -i\omega A_1 &= (-zJ\hbar S + zJ\hbar S\gamma_{\mathbf{k}})A_2, \\ -i\omega A_2 &= (zJ\hbar S - 2K\hbar S y^2 + (1 - 2x^2)zJ\hbar S\gamma_{\mathbf{k}})A_1. \end{aligned} \tag{4.1.5}$$

From these equations, we can construct the following matrix equation:

$$\begin{pmatrix} i\omega & -zJ\hbar S + zJ\hbar S\gamma_{\mathbf{k}} \\ zJ\hbar S - 2K\hbar S y^2 + (1-2x^2)zJ\hbar S\gamma_{\mathbf{k}} & i\omega \end{pmatrix} \begin{pmatrix} A_1 \\ A_2 \end{pmatrix} = 0 \tag{4.1.6}$$

From the determinant of this matrix we can derive the following dispersion relation:

$$\omega_{\mathbf{k}} = z|J|\hbar S\sqrt{(1 - \frac{2Ky^2}{zJ} + (1-2x^2)\gamma_{\mathbf{k}})(1-\gamma_{\mathbf{k}})} \tag{4.1.7}$$

Notice that we found a Goldstone mode, since $\omega_0 = 0$. We find at $\mathbf{k} = 0$ that this corresponds to eigenvectors of the form $(0,1,0,1)^T$. Using the basis of our matrix, it follows that this vector corresponds to a rotation of two neighbouring spins such that they maintain their antiparallel alignment in the xy-plane. This is exactly the symmetry we noticed when we defined our local rotated coordinate system, and it is the symmetry responsible for this Goldstone mode.

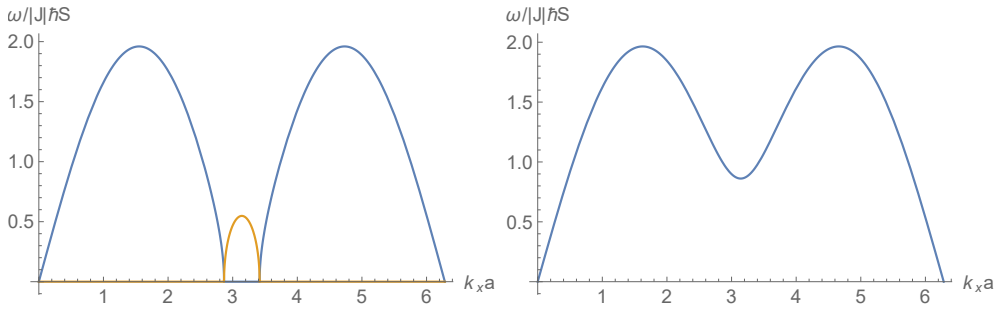

(a) $K/|J| = -0.04$ and $B/|J|\hbar S = 0.25$. **(b)** $K/|J| = -0.04$ and $B/|J|\hbar S = 1$.

Figure 4.2 – Dispersion relations of spin waves for the spin-flop phase for two different values of the magnetic field, for a one-dimensional line. Note for (a) that the blue and yellow curves correspond with the real and imaginary parts of the frequency respectively.

Furthermore, as we find in Figure 4.2a, it follows that the frequency has an imaginary part if the magnetic field B is weak enough. This means that we get exponentially increasing spin waves (for the right values of $\mathbf{k}$), with an eigenvector of the form $(1,0,1,0)^T$. We find that this is a rotation back to the antiferromagnetic phase, compared to our rotated bases. The point where this modes becomes complex is given by $\omega_{\pi/a} = 0$ in the one-dimensional case. This is an equation we can solve for the magnetic field B. Furthermore, this wave vector generalizes as $(\pi/a, \pi/a)^T$ and $(\pi/a, \pi/a, \pi/a)^T$ in the higher-dimensional cases, and we will find that solving those equations will give us the phase transition points between the spin-flop phase and the antiferromagnetic phase.

4.2 Quantum fluctuations in the phase transition point

Now we will work out the Hamiltonian of magnons for the spin-flop state. We will use the same local rotated coordinate systems as in the semi-classical approach. Since we found one set of frequencies in this approach, we will try to diagonalize this Hamiltonian for one set of bosonic operators. First we are going to apply a Holstein-Primakoff transformation on our spin operators in the $\hat{e}_3^A$- and $\hat{e}_3^B$-directions. This gives us:

$$\begin{aligned} H = H_0 + \hbar^2 S\Big((Ky^2 - zJ)\sum_i a_i^\dagger a_i + \frac{1}{2}Ky^2 \sum_i \left(a_i a_i + a_i^\dagger a_i^\dagger\right) \\ + \frac{1}{2}Jx^2 \sum_i \sum_\delta \left(a_i^\dagger a_{i+\delta} + a_i a_{i+\delta}^\dagger\right) - \frac{1}{2}Jy^2 \sum_i \sum_\delta \left(a_i a_{i+\delta} + a_i^\dagger a_{i+\delta}^\dagger\right)\Big), \end{aligned} \tag{4.2.1}$$

where we defined $H_0 = -B\hbar SxN/2 + zJ\hbar^2 S^2 N/2 + K\hbar^2 Sy^2 N/2$.

This Hamiltonian matches the form of Method 1 of Appendix A.2. Thus we can define the following constants $C_1 = \hbar^2 S(Ky^2 - zJ)$, $C_2 = \hbar^2 SJx^2$, $C_3 = \hbar^2 SKy^2$ and $C_4 = -\hbar^2 SJy^2$, which correspond with the constants in front of our summations.
From these constants, we can define the following functions of the wave vector $\mathbf{k}$, namely $A_\mathbf{k} = C_1 + zC_2\gamma_\mathbf{k}$ and $B_\mathbf{k} = C_3 + zC_4\gamma_\mathbf{k}$. These functions match the requirements set by Method 1. Thus we can write down the following diagonalized Hamiltonian:

$$H = E_0 + \sum_\mathbf{k} \hbar\omega_\mathbf{k}(\alpha_\mathbf{k}^\dagger \alpha_\mathbf{k} + \frac{1}{2}), \tag{4.2.2}$$

with $E_0 = H_0 - \frac{1}{2}\sum_\mathbf{k} A_\mathbf{k}$ and $\hbar\omega_\mathbf{k} = \sqrt{A_\mathbf{k}^2 - B_\mathbf{k}^2}$. This frequency $\omega_\mathbf{k}$ is identical to our semi-classical dispersion relation, just as we expected. Now we can analyze the energy for one-dimensional lines, but results generalize similarly for higher-dimensional cases. As we can observe in Figure 4.3, the energy of the spin-flop phase is significantly lower than the energy of the antiferromagnetic phase, for all values of B. However, there is a lower bound for B, and below this bound the ground state energy for the spin-flop phase becomes complex. This is caused by the frequency, since it becomes imaginary for certain values of $\mathbf{k}$, and a sum of the frequency over these values of $\mathbf{k}$ is part of our ground state energy. As we found in the semi-classical approach, these frequencies correspond to exponentially increasing spin waves, rotating to the antiferromagnetic phase. Thus we can argue that the spin-flop phase becomes unphysical due to these magnons, and a phase transition point will occur.

Now we need to determine for which value of B our frequencies become complex. In the one-dimensional case we found that the frequency became imaginary at $k = \pi/a$. Similarly for the higher-dimensional cases, this point is given by $\mathbf{k} = (\pi/a, \pi/a)^T$ or $\mathbf{k} = (\pi/a, \pi/a, \pi/a)^T$, since all these wave vectors correspond with $\gamma_\mathbf{k} = -1$. Now we want to solve $\omega_\mathbf{k} = 0$ for the magnetic field B for these wave vectors. This corresponds to solving $A_\mathbf{k} = \pm B_\mathbf{k}$ for B with $\gamma_\mathbf{k} = -1$. This gives us a complex and a real solution for B. Since complex values for the strength of the magnetic field are unphysical, we get a phase transition at the value $B = 2\hbar S(K - zJ)\sqrt{K/(zJ + K)}$. Compared to the classical phase transition point $B = 2\hbar S\sqrt{K(zJ - K)}$, this means that we get a shift to a slightly lower value of B due to quantum fluctuations. This result is valid for not only the one-dimensional lattice, but also the two- and three-dimensional lattices.

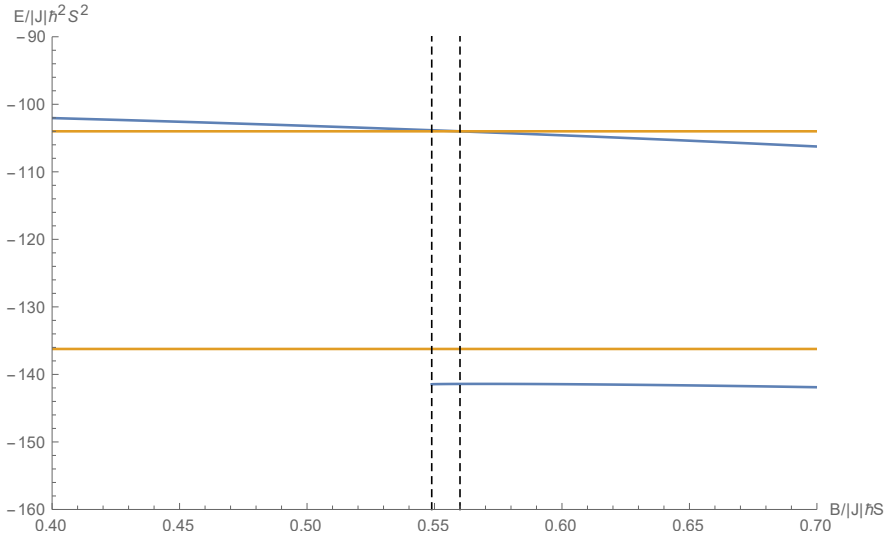

Figure 4.3 – Plot of the energies for $K/|J| = -0.04$, for a one-dimensional lattice. Higher-dimensional lattices give similar curves and crossings. Note that the upper graphs are the classical energies and the lower graphs the energies shifted by quantum fluctuations. Furthermore, the yellow horizontal lines are the antiferromagnetic energies and the blue curves the spin-flop energies.

Chapter 5

Antiferromagnets with DMI

Now we will investigate the influence of the Dzyaloshinskii-Moriya interaction (DMI). This type of interaction is an antisymmetric exchange between neighbouring spins, and was postulated by Dzyaloshinskii [1958] as an explanation for weak ferromagnetism in antiferromagnets. Then Moriya [1960] identified that this interaction is caused by a lack of inversion symmetry in a system, combined with a strong spin-orbit coupling. DMI favours that neighbouring spins are aligned perpendicular to each other, and, depending on the antisymmetric tensor $\mathbf{D}_{ij}$, the spins will form either a clockwise or counterclockwise pattern. In the one dimensional case, this tensor is given by:

$$\mathbf{D}_{ij} = \begin{cases} D\hat{y} & \text{if } j \text{ is the right neighbour of } i, \\ -D\hat{y} & \text{if } j \text{ is the left neighbour of } i, \\ 0 & \text{otherwise.} \end{cases} \tag{5.0.1}$$

This definition generalizes similarly for higher dimensions in the other directions. The sign of this D determines wether the earlier mentioned pattern is clockwise or counterclockwise. In this chapter, we will consider this one-dimensional case for simplicity, and investigate the spiral phase that this interaction induces. In higher dimensions, more complex patterns can be formed by the spins, such as skyrmions.

$$H_{DM} = -\frac{1}{2}\sum_i \sum_\delta \mathbf{D}_{ii+\delta} \cdot \Big(\mathbf{S}_i \times \mathbf{S}_{i+\delta}\Big). \tag{5.0.2}$$

First we will consider a Hamiltonian without anisotropy and no magnetic field, thus $K = 0$ and $B = 0$. We will notice that the energy of this Hamiltonian is minimized for a (cycloidal) spiral, with some wave number that depends on both D and J, which we will investigate in the first paragraph. In the next paragraph we will consider the Hamiltonian with anisotropy and a magnetic field, which will lead to a distortion in the spiral pattern.

5.1 Basics of the Dzyaloshinskii-Moriya interaction

As mentioned, we will take a look at an antiferromagnet with only Heisenberg-exchange interaction and DMI, and we will assume a one-dimensional lattice for convenience. This means the DMI tensor $\mathbf{D}_{ij}$ is given by the expression above. This means that we will deal with the following Hamiltonian in this paragraph:

$$H = -\frac{J}{2}\sum_i \sum_\delta \mathbf{S}_i \cdot \mathbf{S}_{i+\delta} - \frac{D}{2}\sum_i \Big((\mathbf{S}_i \times \mathbf{S}_{i+1})^y - (\mathbf{S}_i \times \mathbf{S}_{i-1})^y\Big). \tag{5.1.1}$$

Now we want to determine the equations we need to solve to minimize our energy. Our ansatz for minimizing the effective energy was a spiral phase. We can argue the existence of this state qualitatively. For two neighbouring spins, the Heisenberg-exchange interaction favours that these spins point in opposite directions, while the DMI favours

that these spins are perpendicular. This means that there is some angle between these spins that minimizes this energy. This angle must be the same for all neighbouring spins, and this causes an (alternating) spiral pattern. Thus, we get a spiral wave with an angle $aq + \pi$ between neighbouring spins, where q is the wave number of our spiral and a our lattice constant, and we add π to induce an alternating pattern. This gives us the following ansatz for our spin vector:

$$\mathbf{S}_i/\hbar S = \sin(aqi + \pi i)\hat{x} + \cos(aqi + \pi i)\hat{z}. \tag{5.1.2}$$

Then the classical energy is given by $E^{spiral} = J\cos(aq) + D\sin(aq)$ per spin. This energy is minimized for the angle $aq = \arctan[D/J]$. Our minimized energy per spin is given by $E^{spiral} = -\sqrt{J^2 + D^2}\hbar^2 S^2$. For a regular antiferromagnet, the minimal energy is given by $E^{AFM} = J\hbar^2 S^2$. Thus we find that these energies are equal at $D = 0$, and for this value we find indeed that our spiral forms an antiferromagnetic configuration ($aq = 0$). For other values of D, the energy of our spiral phase is lower compared to the antiferromagnetic phase, and is thus the preferred state. Note that all these results are quite similar for ferromagnets, with as difference that the spiral moves in the other direction.

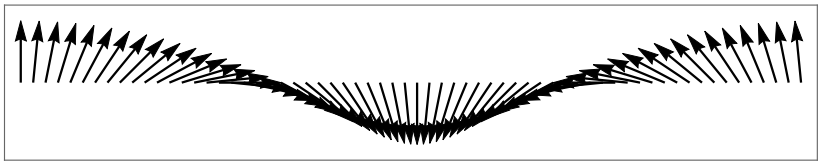

(a) Spiral phase for a ferromagnet.

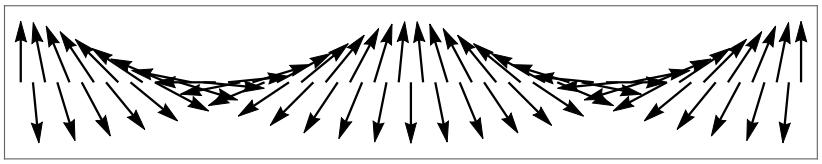

(b) Spiral phase for an antiferromagnet.

Figure 5.1 – Graphical depiction of spiral phases for both types of magnets. Both for 64 spins with $D/|J| = 0.0984914$.

Now we will look at spin waves through the spiral phase. In a similar fashion as in the previous chapters, we can derive the equations of motion for the deviations of a spin at site i by using the equation following from Ehrenfest's theorem. Note that the partial derivative is a bit different for the DMI-term, since it involves a cross product instead of an inner product. To be able to work this out, we need to define local rotated coordinate systems corresponding with $\theta_i = aqi + \pi i$ and $\phi_i = 0$. Furthermore, it turns out that it is sufficient to make one general plane-wave ansatz for our spins. Altogether, this gives us the following matrix equation for the amplitudes:

$$\begin{pmatrix} i\omega & 2\hbar S\big(\sqrt{J^2 + D^2} - J\cos(ka)\big) \\ -2\hbar S\sqrt{J^2 + D^2}\big(1 - \cos(ka)\big) & i\omega \end{pmatrix} \begin{pmatrix} A_1 \\ A_2 \end{pmatrix} = 0. \tag{5.1.3}$$

We can derive the following dispersion relation from the determinant equation of this matrix:

$$\omega_k = 2\hbar S\sqrt{J^2 + D^2}\sqrt{\left(1 - \frac{J}{\sqrt{J^2 + D^2}}\cos(ka)\right)\Big(1 - \cos(ka)\Big)}. \tag{5.1.4}$$

This mode is a Goldstone mode, corresponding to the symmetry that we could have started a spiral at any site, and thus that we can rotate all spins with the same angle around the $\hat{y}$-axis.

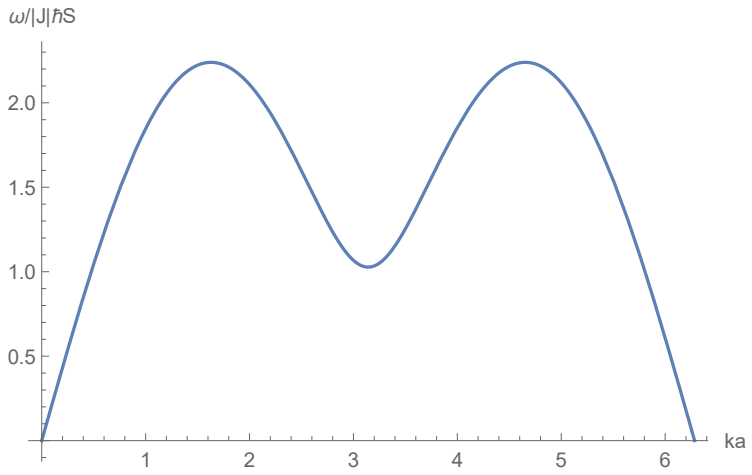

Figure 5.2 – Dispersion relation for the regular spiral phase, with $D/|J| = 0.5$.

Now we can examine the quantum-mechanical Hamiltonian of magnons for this spiral phase. Using the same local rotated coordinate systems as before, and applying a Holstein-Primakoff transformation as described in Appendix A.1 for these axes, we can write down the following Hamiltonian:

$$\begin{aligned} H =& H_0 + 2\sqrt{J^2+D^2}\hbar^2 S \sum_i a_i^\dagger a_i \\ &- \frac{1}{4}\left(J+\sqrt{J^2+D^2}\right)\hbar^2 S \sum_i \sum_\delta \left(a_i a_{i+\delta}^\dagger + a_i^\dagger a_{i+\delta}\right) \\ &+ \frac{1}{4}\left(J-\sqrt{J^2+D^2}\right)\hbar^2 S \sum_i \sum_\delta \left(a_i a_{i+\delta} + a_i^\dagger a_{i+\delta}^\dagger\right), \end{aligned} \tag{5.1.5}$$

where we defined $H_0 = -N\hbar^2 S^2\sqrt{J^2+D^2}$. We can follow Method 1 and set $C_1 = 2\sqrt{J^2+D^2}\hbar^2 S$, $C_2 = -(J+\sqrt{J^2+D^2})/2$, $C_3 = 0$ and $C_4 = (J-\sqrt{J^2+D^2})/2$.

Then we can define the functions $A_k = C_1 + 2C_2\cos(ka)$ and $B_k = 2C_4\cos(ka)$ from these constants. This gives us the frequency $\hbar\omega_k = \sqrt{A_k^2 - B_k^2}$, which is identical to the dispersion relation from the semi-classical approach. Furthermore, we get the following diagonalized Hamiltonian:

$$H = E_0 + \sum_k \hbar\omega_k(\alpha_k^\dagger\alpha_k + \frac{1}{2}), \tag{5.1.6}$$

with $E_0 = H_0 - \frac{1}{2}\sum_k A_k$.

Now we will conclude this paragraph with a short note on the effect of DMI for antiferromagnetic or spin-flop configurations. Due to the alternating pattern of both configurations, it turns out that the contribution to the semi-classical energy by DMI is zero. Similarly, the DMI sum of the quantum-mechanical Hamiltonian vanishes, when we transform our spin operators as we did in Chapters 3 and 4. This means that our results from these chapters are still valid when we consider a Hamiltonian with DMI, and we do not need to perform any new calculations to compare these states to the spiral phase. Up front, we could have expected this, since both these configurations have inversion symmetry, while DMI is restricted to systems that lack inversion symmetry.

5.2 Magnetic frustration of the spiral phase

In this paragraph we consider the effects of anisotropy and a magnetic field on the spiral phase. Anisotropy favours that the spins point in the $\pm\hat{z}$-directions, while the magnetic field only favours the $+\hat{z}$-direction. These interactions cause a magnetic frustration in our spin lattice, i.e. the spins can not satisfy every interaction simultaneously. For our system, this means that our spins will form a spiral pattern, but deviate slightly to favour these other interactions. However, we will not be able to develop an analytical solution to describe these deviations, since problems involving magnetic frustration are, simply put, too complicated for this. A good starting point is linearizing the equations involving this frustration, and either use an ansatz which approximates these equations, or solve them numerically. Later on we will use the insights that we get from this approach to calculate the deviations quite accurately.

$$\begin{aligned} H = &-\frac{J}{2}\sum_i\sum_\delta \mathbf{S}_i\cdot\mathbf{S}_{i+\delta} - \frac{1}{2}\sum_i\sum_\delta \mathbf{D}_{ii+\delta}\cdot\Big(\mathbf{S}_i\times\mathbf{S}_{i+\delta}\Big) \\ &- B\sum_i \mathbf{S}_i\cdot\hat{z} + K\sum_i\Big(\mathbf{S}_i\cdot\hat{z}\Big)^2. \end{aligned} \tag{5.2.1}$$

We can describe the deviations from the regular spiral phase by the angles $\delta\theta_i$, which are still unknown. Then the vector of our spin is described by:

$$\mathbf{S}_i/\hbar S = \sin(aqi+\pi i+\delta\theta_i)\hat{x} + \cos(aqi+\pi i+\delta\theta_i)\hat{z}. \tag{5.2.2}$$

We can fill these vectors in into our Hamiltonian (Equation 5.2.1). This gives us the following classical energy for our system:

$$\begin{aligned} E^{total} = &-\frac{1}{2}\sqrt{J^2+D^2}\hbar^2S^2\sum_i\Big(\cos(\delta\theta_{i+1}-\delta\theta_i)+\cos(\delta\theta_i-\delta\theta_{i-1})\Big) \\ &- B\hbar S\sum_i\cos(aqi+\pi i+\delta\theta_i) + K\hbar^2S^2\sum_i\cos^2(aqi+\delta\theta_i). \end{aligned} \tag{5.2.3}$$

Now we want to minimize this classical energy. Compared to our previous phases, it is not possible to construct a general energy per spin for the spiral phase. Thus, we must minimize our total classical energy for each deviation $\delta\theta_j$. This yields the following set of equations:

$$\begin{aligned} \sqrt{J^2+D^2}\Big(\sin(\delta\theta_j-\delta\theta_{j+1})+\sin(\delta\theta_j-\delta\theta_{j-1})\Big) =& K\sin(2aqj+2\delta\theta_j) \\ &- \frac{B}{\hbar S}\sin(aqj+\pi j+\delta\theta_j). \end{aligned} \tag{5.2.4}$$

Note that the factor $1/2$ on the left side disappears, since each term in the nearest neighbour sum appears twice. This gives us a set of N non-linear equations. By assuming periodic boundary conditions, we have N variables $\delta\theta_i$ for which we want to solve these equations. The regular antiferromagnetic phase (which corresponds with $\delta\theta_i = -aqi$) solves these equations. Similarly, it is quite possible that there are many more solutions to this set of equations, due to the large number of variables and equations. Some of these solutions can even be maxima, since we are only certain that we determine extrema with this method. Therefore each of the solutions to this set of equations can be correct, but also quite far off in minimizing the energy absolutely.

It turns out that numerical solutions to these non-linear equations are an example of this type of useless solutions. First of all, they do not lower the total energy below the energy of the regular spiral phase. Second, the angles that we calculate with this method seem rather unphysical, i.e. the deviations are sometimes in favour of anisotropy and the magnetic field, and sometimes at expense of these interactions. Altogether, we can conclude that this set of non-linear equations will not provide a good solution consistently. Therefore, we will linearize these equations.

Since the anisotropy is typically weak, i.e. $|K| \ll \sqrt{J^2 + D^2}$, we expect that the deviation with respect to the spiral phase due to this interaction will be small too. Similarly, if we will only consider weak magnetic fields, i.e. $B \ll \hbar S\sqrt{J^2 + D^2}$, the deviation due to this interaction will be small too. Thus, we can linearize our equations in $\delta\theta_i$, which gives us the following set of equations:

$$\begin{aligned} 2\delta\theta_j =& \delta\theta_{j+1} + \delta\theta_{j-1} + x\sin(2aqj) + 2x\cos(2aqj)\delta\theta_j \\ & - y\sin(aqj + \pi j) - y\cos(aqj + \pi j)\delta\theta_j, \end{aligned} \tag{5.2.5}$$

where we defined the dimensionless constants $x = K/\sqrt{J^2 + D^2}$ and $y = B/(\hbar S\sqrt{J^2 + D^2})$. This is a set of equations that we can solve numerically. However, we can find an approximate solution by some physical arguments. Since we assume that the anisotropy and the magnetic field are weak, we know that x and y must be small. We also argued that the corresponding deviations $\delta\theta_i$ must be small. This means that we can neglect terms involving both a factor x or y, and the deviation $\delta\theta_i$. Then our equation reduces to:

$$2\delta\theta_j = \delta\theta_{j+1} + \delta\theta_{j-1} + x\sin(2aqj) - y\sin(aqj + \pi j). \tag{5.2.6}$$

Now we can split our deviation into two parts, one due to anisotropy and one due to the magnetic field. By our approximation in the equation above, any interaction between these parts can be neglected. The basic idea is that the deviation due to the magnetic field is always towards the $+\hat{z}$-direction, whereas the deviation due to the anisotropy depends on wether the spin points up or down. Furthermore, it is likely that these deviations behave as a wave, since the influence of the deviation varies with the position in the spiral wave. This behaviour has been summarized in Figure 5.3. Note that, when we do not neglect the other two terms, more waves in the form of higher order harmonics will be needed to describe our solutions, and a coupling between the two interactions will arise.

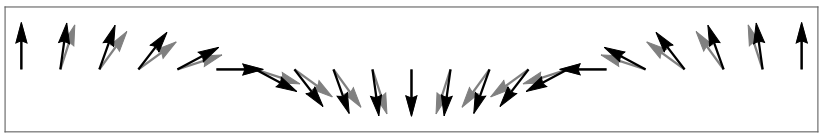

(a) Spiral phase for a ferromagnet, frustrated by anisotropy.

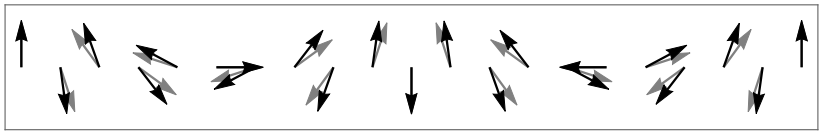

(b) Spiral phase for an antiferromagnet, frustrated by anisotropy.

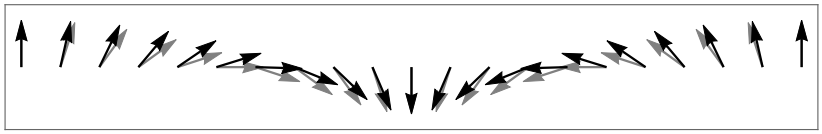

(c) Spiral phase for a ferromagnet, frustrated by a magnetic field.

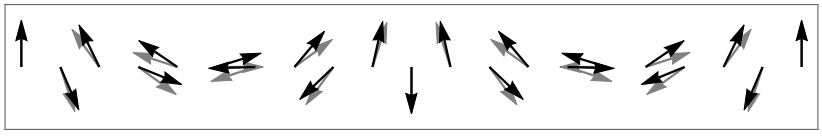

(d) Spiral phase for an antiferromagnet, frustrated by a magnetic field.

Figure 5.3 – Graphical depiction of frustrated spiral phases for both types of magnets, now for 20 spins with $D/|J| = 0.32492$. Note that the original alignment is shown by the gray arrows, while the frustrated alignment is shown by the black arrows.

Following the previous arguments, we can use a superposition of two waves to describe the frustration through our spin configuration. This ansatz is given by $\delta\theta_i = X\sin(2aqi) + Y\sin(aqi + \pi i)$, where X, Y are the amplitudes of both waves. Note that these two sines are identical to the sines in the equation, and that both show exactly the behaviour we expect for the deviations. When we plug this ansatz into Equation 5.2.6, we find the amplitudes $X = x/[2(1-\cos(2aq))]$ and $Y = -y/[2(1+\cos(aq))]$. When we compare this approximated ansatz to numerical results for Equation 5.2.5, we find that both methods give similar results.

Furthermore, we see that these solutions do lower the ground state energy compared with the regular spiral phase. However, when the magnetic field is strong, our linearization is no longer valid, and this energy could be minimized more effectively. Therefore we can use this ansatz $\delta\theta_i = X\sin(2aqi) + Y\sin(aqi + \pi i)$, and derive the following two equations by minimizing the total energy for the amplitudes X, Y:

$$\frac{\partial E^{total}}{\partial X} = 0, \text{ and } \frac{\partial E^{total}}{\partial Y} = 0. \tag{5.2.7}$$

Now we have two non-linear equations, and two unknown variables. It turns out that numerical solutions to these equations do minimize the ground state energy more effectively.[1] We can use these solutions to develop a phase diagram between the spin-flop phase, the antiferromagnetic phase and the spiral phase in the (B, D)-plane, where we can use our analytical results for the first two phases.

This phase diagram is given in Figure 5.4. Note that we acquired this phase diagram by assuming periodic boundary conditions and spirals of integer length. For a given set of values for the magnetic field $B/|J|\hbar S$, we varied the length of these spirals (and thus the value $D/|J|$) to match the energy of the antiferromagnetic phase or the spin-flop phase. This explains the rather discrete behaviour of our phase diagram for large values of $D/|J|$, since this domain corresponds to short spirals. However, it is an effective method to describe the phase diagram for low values of $D/|J|$, which is a more interesting domain, since it suggests a triple point between our phases. Furthermore, we only considered odd spirals when the magnetic field is non-zero, since the magnetic field favours that spirals have a net magnetic moment.

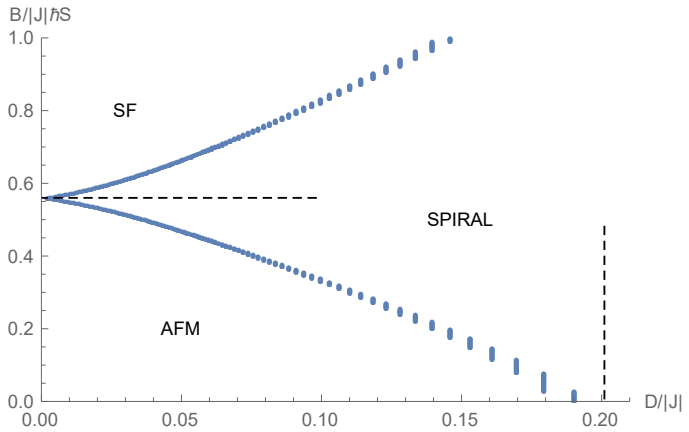

Figure 5.4 – Ground state phase diagram of a one-dimensional antiferromagnet, for the antiferromagnetic phase (AFM), the spin-flop phase (SF) and the spiral phase (SPIRAL). Furthermore we set the anisotropy to $K/|J| = -0.04$. Note that the original AFM-SPIRAL and AFM-SF phase transitions are visualised by dashed lines.

[1] Note that we should divide both equations by $\sqrt{J^2 + D^2}\hbar^2 S^2$ (or another constant) to make the equation dimensionless and suitable for numerical computations.

Chapter 6

Conclusion and discussion

6.1 Conclusion

In the first part of this thesis we analyzed the influence of quantum fluctuations on magnetic configurations, and compared these results to a semi-classical analysis. We found that quantum fluctuations lower the ground state energy for an antiferromagnetic configuration, and that this configuration has two different kind of magnons. Furthermore, we found that one type of these magnons has negative eigenvalues for high values of the magnetic field strength B. When we analyzed the spin-flop phase, we noticed that this phase is preferred when these magnons exist, i.e. the phase transition to the spin-flop state occurs for a lower value of the magnetic field strength B. We also found that quantum fluctuations lower the energy of this spin-flop phase, such that phase transition point to the antiferromagnetic phase is shifted to a slightly lower value of B.

Then we considered a Hamiltonian with Dzyaloshinskii-Moriya interaction. Without a magnetic field and anisotropy, this causes a spiral pattern. We found that quantum fluctuations do not influence this phase, and the phase transition to the antiferromagnetic case always occurs when the DMI is zero. When we did consider these interactions, we argued that both interactions cause a frustration to this pattern. We found a useful description of this frustration from a linearization, which we used to develop a ground state phase diagram between the antiferromagnetic phase, the spin-flop phase and the spiral phase. This diagram suggested a triple point when the DMI is zero, at the phase transition point between the antiferromagnetic phase and the spin-flop phase.

Combining these results, we expect that either the triple point is slightly shifted due to quantum fluctuations, or that it is divided into two seperate phase transitions. Since we couldn't determine the effect of quantum fluctuations on the spiral phase, we do not know which case holds, and we will discuss this in the next paragraph.

6.2 Discussion and suggestions for future research

The first questionable result we found was the existence of magnons with negative eigenvalues in the antiferromagnetic phase. We found that these exist for high values of the magnetic field B, where we expect the spin-flop phase. Arguing from the antiferromagnetic phase, we could add these magnons until the ground state energy is lower than the spin-flop energy. However, when we consider magnons in a ground state, we should at least take magnon-magnon interactions into consideration, since these do influence the energy. This can be done by including bosonic operators up to fourth order, when we apply the Holstein-Primakoff transformation. The expected result is that these magnon-magnon interactions cancel the negative eigenvalues at least partly, such that the spin-flop state remains the preferred configuration. However, this is just speculation and could be investigated in the future.

Then we found that quantum fluctuations lower the strength of the magnetic field B for the phase transition between the antiferromagnetic phase and the spin-flop phase. However, we noticed that the ground state energy of the spin-flop phase was still lower at this point, and that this phase transition was induced by the fact that this energy became complex, instead of an energy crossing.

First of all, the fact that this ground state energy is complex, means that this state is unphysical, since physical states have real energies.
Second, we found that the imaginary part of the energy was caused by the imaginary eigenvalues for magnons. These eigenvalues correspond to exponentially increasing (semi-classical) spin waves, which rotate to the antiferromagnetic phase. This explains the phase transition from a semi-classical point of view.
At last, we applied a numerical analysis on both states, using an algorithm developed by van Dieten [2015]. We found that this analysis agrees with our analytical results, which has been included in Appendix A.4. Combining these arguments, we can be certain of the correctness of our calculation and the interpretation of these results.

Then we considered the Dzyaloshinskii-Moriya interaction, and constructed a phase diagram by only using spirals of integer length. Furthermore, we used an ansatz that was derived in an approximation where the magnetic field was weak, and used this for all values of the magnetic field.

For both points we need to remember that they still describe spirals, and it only causes our subset of all possible spiral configurations to become smaller. This means that the suggestion for a triple point is still valid, but that the area for the spiral phase would be larger if we could consider more spiral configurations. Optimizing our model for the magnetic frustration is therefore a good starting point for future research. Using higher order harmonics in the deviation due to the magnetic field, which we neglected in Chapter 5, is one way this could be achieved.

Another method for developing this phase diagram is considering a fixed number of spins, and vary $D/|J|$ for this lattice instead of the integer length of the spirals. This way, we would get more accurate results in the high $D/|J|$-regime. However, it also means that our spiral pattern is not always periodic on the boundaries, which means that our numerical computation of the amplitudes is no longer possible, since it relies on this periodicity. Furthermore, the length of our spirals should be negligible compared to the number of spins (since there is an unfinished spiral at the end our lattice), which causes another difficulty for our numerical computations, since the typical length of spirals in the low $D/|J|$-regime is ~ 1000 spins.

At last, we tried a numerical approach to quantum fluctuations in the frustrated spiral phase (using the method of van Dieten [2015]), which has not been included in this thesis. We couldn't develop a useful algorithm to make a phase diagram of these fluctuations, because the energies of the spiral configuration were not consistent. With this we mean that the energies for most spiral configurations were complex, and that this imaginary part could not be neglected. This suggests that our configurations are unphysical in the quantum-mechanical sense, which is probably due to the fact that our model for the frustration is only an approximation. Again, optimizing this model could solve this problem. Furthermore, for completeness, we have included an analytical approach to diagonalize the Hamiltonian for general unknown deviations in Appendix A.2. This could be used in the case that an analytical description for the frustration has been derived.

Appendix A

Derivations, identities and numerical results

In this appendix we will explain concepts and methods that we used in this thesis. In the first section we will introduce some general concepts such as rotated coordinate systems and general Holstein-Primakoff transformations. In the next section we will give some general derivations and methods to diagonalize the Hamiltonian for spin lattices, including an attempt to diagonalize the Hamiltonian for the frustrated spiral phase. We will try to keep our results in these section as general as possible. Then, in the third section, we will give a list of equations that we used in this thesis, each of which we supply with a short explanation or derivation. In the last section we include a comparison between our analytical results on the ground state energy for the spin-flop and antiferromagnetic configuration, and numerical computations of these energies.

A.1 Mathematical concepts

To describe the direction and components of our spin, we introduce a local rotated coordinate system. The direction of the spin at site i is given by $\hat{e}_3^i$, and described by the polar angle θ_i and the azimuthal angle ϕ_i. This rotated coordinate system is given by the following expressions:

$$\begin{aligned}\hat{e}_1^i &= \cos\theta_i \cos\phi_i \hat{x} + \cos\theta_i \sin\phi_i \hat{y} - \sin\theta_i \hat{z},\\ \hat{e}_2^i &= \hat{e}_3^i \times \hat{e}_1^i,\\ \hat{e}_3^i &= \sin\theta_i \cos\phi_i \hat{x} + \sin\theta_i \sin\phi_i \hat{y} + \cos\theta_i \hat{z}.\end{aligned} \tag{A.1.1}$$

For certain lattices it could be useful to split this up for two different sublattices A and B, which could be expressed as $i = A, B$. This is useful for both the semi-classical and the quantum-mechanical approach, and we used this method for the antiferromagnetic configuration in Chapter 3. Then, for the semi-classical approach, it is useful to let spin vectors deviate from their initial alignment along $\hat{e}_3$. This can be expressed as:

$$\mathbf{S}_j = \delta S_j^1 \hat{e}_1^j + \delta S_j^2 \hat{e}_2^j + \hbar S \hat{e}_3^j. \tag{A.1.2}$$

If necessary, we can couple the position j to a sublattice A or B, just like for the rotated coordinate system. A good ansatz for spin waves is then given by:

$$\delta S_j^i = A_i \exp[i(\mathbf{k}\cdot\mathbf{r}_j - \omega t)] \text{ for } i = 1, 2, \tag{A.1.3}$$

where A_i is the amplitude of the deviations of the spin for the two components $i = 1, 2$, $\mathbf{k}$ is the wave vector of the spin wave, and ω the frequency. Note that multiple spins can have the same amplitude for their components, while their phase factor (the complex exponential) is different. In general we should only use different amplitudes for spins, if they belong to different sublattices. This concludes all the mathematics needed for a semi-classical approach.

In the quantum-mechanical approach, one can express the Holstein-Primakoff transformation as the following transformation for the components of a spin operator:

$$\begin{aligned} S_i^1 &= \hbar\sqrt{\frac{S}{2}}(a_i + a_i^\dagger), \\ S_i^2 &= -i\hbar\sqrt{\frac{S}{2}}(a_i - a_i^\dagger), \\ S_i^3 &= \hbar(S - a_i^\dagger a_i), \end{aligned} \tag{A.1.4}$$

where we used $S_i^\pm = S_i^1 \pm iS_i^2$ and the regular Holstein-Primakoff transformation for the spin lowering and raising operator. Furthermore, the spin operator at site i can be written as $\mathbf{S}_i = S_i^1\hat{e}_i^1 + S_i^2\hat{e}_i^2 + S_i^3\hat{e}_i^3$. Now we have all the mathematics needed to write out our Hamiltonian in bosonic operators.

A.2 Analytical diagonalization of the Hamiltonian

In this paragraph we will start with two general expressions for the Hamiltonian, and diagonalize it using both Fourier transformations and Bogoliubov transformations. The basic idea is to choose our transformation in such a way, that our off-diagonal terms vanish, while maintaining the bosonic operator relations (Stoof et al. [2009]). This can be accomplished by letting our transformation depend on two functions $u_\mathbf{k}$ and $v_\mathbf{k}$, that depend on the wave vector $\mathbf{k}$.

Method 1

Suppose we start with a general Hamiltonian of the following form:

$$\begin{aligned} H =& H_0 + \sum_i C_1 a_i^\dagger a_i + \frac{1}{2}\sum_i\sum_\delta C_2\Big(a_i^\dagger a_{i+\delta} + a_i a_{i+\delta}^\dagger\Big) \\ &+ \frac{1}{2}\sum_i C_3\Big(a_i a_i + a_i^\dagger a_i^\dagger\Big) + \frac{1}{2}\sum_i\sum_\delta C_4\Big(a_i a_{i+\delta} + a_i^\dagger a_{i+\delta}^\dagger\Big), \end{aligned} \tag{A.2.1}$$

where it is important that our constants C_1, C_2, C_3, C_4 do not depend on the position i. Otherwise, some identities for the Fourier transformation, as given in Equation A.3.2, would not work, which brings us to our next step. We want to apply a Fourier transformation according to $a_j = \sum_\mathbf{k} e^{i\mathbf{k}\cdot\mathbf{r}_j} a_\mathbf{k}$. This yields the following Hamiltonian:

$$\begin{aligned} H =& H_0 + \sum_\mathbf{k} C_1 a_\mathbf{k}^\dagger a_\mathbf{k} + \sum_\mathbf{k} zC_2\gamma_\mathbf{k} a_\mathbf{k}^\dagger a_\mathbf{k} \\ &+ \frac{1}{2}\sum_\mathbf{k} C_3\Big(a_\mathbf{k} a_{-\mathbf{k}} + a_\mathbf{k}^\dagger a_{-\mathbf{k}}^\dagger\Big) + \frac{1}{2}\sum_\mathbf{k} zC_4\gamma_\mathbf{k}\Big(a_\mathbf{k} a_{-\mathbf{k}} + a_\mathbf{k}^\dagger a_{-\mathbf{k}}^\dagger\Big), \end{aligned} \tag{A.2.2}$$

where we defined $z\gamma_\mathbf{k} = \sum_\mathbf{k}\cos(\mathbf{k}\cdot\delta)$. To be able to do this, we used Equations A.3.1 and A.3.2. Now, by writing $A_\mathbf{k} = C_1 + zC_2\gamma_\mathbf{k}$ and $B_\mathbf{k} = C_3 + zC_4\gamma_\mathbf{k}$, we can simplify our Hamiltonian as:

$$H = H_0 + \sum_\mathbf{k} A_\mathbf{k} a_\mathbf{k}^\dagger a_\mathbf{k} + \frac{1}{2}\sum_\mathbf{k} B_\mathbf{k}\Big(a_\mathbf{k} a_{-\mathbf{k}} + a_\mathbf{k}^\dagger a_{-\mathbf{k}}^\dagger\Big). \tag{A.2.3}$$

Now we can apply the Bogoliubov transformation $a_\mathbf{k} = u_\mathbf{k}\alpha_\mathbf{k} + v_\mathbf{k}\alpha_{-\mathbf{k}}^\dagger$, where we have $u_\mathbf{k} = \cosh\theta_\mathbf{k}$ and $v_\mathbf{k} = \sinh\theta_\mathbf{k}$ as our functions of $\mathbf{k}$, with $\theta_\mathbf{k} = \theta_{-\mathbf{k}}$. We force these conditions to ensure that our new operator $\alpha_\mathbf{k}$ obeys the boson commutation relations $[\alpha_\mathbf{k}, \alpha_{\mathbf{k}'}^\dagger] = \delta_{\mathbf{k}\mathbf{k}'}$ and $[\alpha_\mathbf{k}, \alpha_{\mathbf{k}'}] = [\alpha_\mathbf{k}^\dagger, \alpha_{\mathbf{k}'}^\dagger] = 0$, as is required for Bogoliubov transformations. Later on we will see that, because $\theta_\mathbf{k}$ needs to be symmetric, that $A_\mathbf{k}$ and $B_\mathbf{k}$ both need to be symmetric. This is indeed the case, since $\gamma_\mathbf{k}$ is symmetric. Using hyperbolic

trigonometric identities for our functions $u_{\mathbf{k}}$ and $v_{\mathbf{k}}$, we can rewrite our Hamiltonian as:

$$\begin{aligned} H = H_0 - \frac{1}{2}\sum_{\mathbf{k}} A_{\mathbf{k}} + \sum_{\mathbf{k}} \Big(A_{\mathbf{k}}(u_{\mathbf{k}}^2 + v_{\mathbf{k}}^2) + B_{\mathbf{k}} 2u_{\mathbf{k}}v_{\mathbf{k}}\Big)(\alpha_{\mathbf{k}}^\dagger \alpha_{\mathbf{k}} + \frac{1}{2}) \\ + \frac{1}{2}\sum_{\mathbf{k}} \Big(A_{\mathbf{k}} 2u_{\mathbf{k}}v_{\mathbf{k}} + B_{\mathbf{k}}(u_{\mathbf{k}}^2 + v_{\mathbf{k}}^2)\Big)(\alpha_{\mathbf{k}}\alpha_{-\mathbf{k}} + \alpha_{\mathbf{k}}^\dagger \alpha_{-\mathbf{k}}^\dagger). \end{aligned} \tag{A.2.4}$$

This means that we get the following restriction to diagonalize our Hamiltonian:

$$\tanh 2\theta_{\mathbf{k}} = -\frac{B_{\mathbf{k}}}{A_{\mathbf{k}}}. \tag{A.2.5}$$

As mentioned, from this equation we see that, because $\theta_{\mathbf{k}}$ must be symmetric, both $A_{\mathbf{k}}$ and $B_{\mathbf{k}}$ must be symmetric (or antisymmetric). Using this equation, we get the following Hamiltonian:

$$H = E_0 + \sum_{\mathbf{k}} \hbar\omega_{\mathbf{k}} \Big(\alpha_{\mathbf{k}}^\dagger \alpha_{\mathbf{k}} + \frac{1}{2}\Big), \tag{A.2.6}$$

where we defined $E_0 = H_0 - \frac{1}{2}\sum_{\mathbf{k}} A_{\mathbf{k}}$ and $\hbar\omega_{\mathbf{k}} = \sqrt{A_{\mathbf{k}}^2 - B_{\mathbf{k}}^2}$. In Appendix A.3 we included a calculation of this frequency.

Method 2

Now suppose our Hamiltonian doesn't match the required form of Method 1. That is, some constants do depend on the position i, and, to be more specific, on which sublattice i belongs to. We can fix this problem by splitting the lattice in two sublattices A and B with boson operators a_i and b_i. Then we can apply a Fourier transformation on these operators, and write the Hamiltonian in the following form:

$$\begin{aligned} H =& H_0 + \sum_{\mathbf{k}} A_{\mathbf{k}} \Big(a_{\mathbf{k}}^\dagger a_{\mathbf{k}} + b_{\mathbf{k}}^\dagger b_{\mathbf{k}}\Big) + \sum_{\mathbf{k}} B_{\mathbf{k}} \Big(a_{\mathbf{k}} b_{-\mathbf{k}} + a_{\mathbf{k}}^\dagger b_{-\mathbf{k}}^\dagger\Big) \\ &+ \sum_{\mathbf{k}} C_{\mathbf{k}}(a_{\mathbf{k}}^\dagger a_{\mathbf{k}} - b_{\mathbf{k}}^\dagger b_{\mathbf{k}}). \end{aligned} \tag{A.2.7}$$

Here, this last sum is caused by the fact that some of our original constants did depend on the lattice site i. Now we are going to apply a Bogoliubov transformation according to $a_{\mathbf{k}} = u_{\mathbf{k}}\alpha_{\mathbf{k}} + v_{\mathbf{k}}\beta_{-\mathbf{k}}^\dagger$ and $b_{\mathbf{k}} = u_{\mathbf{k}}\beta_{\mathbf{k}} + v_{\mathbf{k}}\alpha_{-\mathbf{k}}^\dagger$. Once again, we have $u_{\mathbf{k}} = \cosh\theta_{\mathbf{k}}$ and $v_{\mathbf{k}} = \sinh\theta_{\mathbf{k}}$, with $\theta_{\mathbf{k}} = \theta_{-\mathbf{k}}$, to enforce the commutation relations. As we will see later, we want again for $A_{\mathbf{k}}$ and $B_{\mathbf{k}}$ to be symmetric to get a symmetric $\theta_{\mathbf{k}}$. [1] Applying this transformation, we get the following Hamiltonian:

$$\begin{aligned} H = H_0 - \sum_{\mathbf{k}} A_{\mathbf{k}} + \sum_{\mathbf{k}} \Big(A_{\mathbf{k}}(u_{\mathbf{k}}^2 + v_{\mathbf{k}}^2) + B_{\mathbf{k}} 2u_{\mathbf{k}}v_{\mathbf{k}}\Big)(\alpha_{\mathbf{k}}^\dagger \alpha_{\mathbf{k}} + \frac{1}{2} + \beta_{\mathbf{k}}^\dagger \beta_{\mathbf{k}} + \frac{1}{2}) \\ \sum_{\mathbf{k}} \Big(A_{\mathbf{k}} 2u_{\mathbf{k}}v_{\mathbf{k}} + B_{\mathbf{k}}(u_{\mathbf{k}}^2 + v_{\mathbf{k}}^2)\Big)(\alpha_{\mathbf{k}}\beta_{-\mathbf{k}} + \alpha_{\mathbf{k}}^\dagger \beta_{-\mathbf{k}}^\dagger) + \sum_{\mathbf{k}} C_{\mathbf{k}}(\alpha_{\mathbf{k}}^\dagger \alpha_{\mathbf{k}} - \beta_{\mathbf{k}}^\dagger \beta_{\mathbf{k}}). \end{aligned} \tag{A.2.8}$$

This gives us the following solution to diagonalize our Hamiltonian:

$$\tanh 2\theta_{\mathbf{k}} = -\frac{B_{\mathbf{k}}}{A_{\mathbf{k}}}. \tag{A.2.9}$$

This equation is identical to Method 1. Then we can write out our Hamiltonian as:

$$H = E_0 + \sum_{\mathbf{k}} \hbar\omega_{\mathbf{k}}^+ \Big(\alpha_{\mathbf{k}}^\dagger \alpha_{\mathbf{k}} + \frac{1}{2}\Big) + \sum_{\mathbf{k}} \hbar\omega_{\mathbf{k}}^- \Big(\beta_{\mathbf{k}}^\dagger \beta_{\mathbf{k}} + \frac{1}{2}\Big), \tag{A.2.10}$$

with $E_0 = H_0 - \sum_{\mathbf{k}} A_{\mathbf{k}}$ and $\hbar\omega_{\mathbf{k}}^\pm = \sqrt{A_{\mathbf{k}}^2 - B_{\mathbf{k}}^2} \pm C_{\mathbf{k}}$. When calculating these values, and especially these sums over $\mathbf{k}$, one should remember that it is caused by our Fourier transformation of a_i and b_i, so it is a sum over $N/2$ terms instead of N terms, which was the case in Method 1.

[1] We want $C_{\mathbf{k}}$ to be symmetric too, so that some cross terms will cancel out to make the diagonalization easier.

Hamiltonian for the frustrated spiral phase

Now we will provide an expression for the Hamiltonian of the frustrated spiral phase, for the (general) angles $\theta_i = aqi + \pi i + \delta\theta_i$ (and $\phi_i = 0$). We used the corresponding local rotated coordinate systems and applied Holstein-Primakoff transformations to describe our spin operators. This gave us the following expression:

$$\begin{aligned}
H =& -\frac{1}{2}\hbar^2 S^2\sqrt{J^2+D^2}\sum_i(\cos(\delta\theta_{i+1}-\delta\theta_i)+\cos(\delta\theta_{i-1}-\delta\theta_i))\\
&+K\hbar^2S^2\sum_i\cos^2(aqi+\delta\theta_i)+K\hbar^2\frac{S}{2}\sum_i\sin^2(aqi+\delta\theta_i)\\
&-B\hbar S\sum_i\sin(aqi+\pi i+\delta\theta_i)\\
&+\hbar^2S\sum_i a_i^\dagger a_i\Bigg(\sqrt{J^2+D^2}(\cos(\delta\theta_{i+1}-\delta\theta_i)+\cos(\delta\theta_{i-1}-\delta\theta_i))\\
&+\frac{1}{2}K(1-3\cos^2(aqi+\delta\theta_i))+\frac{B}{\hbar S}\cos(aqi+\pi i+\delta\theta_i)\Bigg)\\
&-\frac{1}{4}\hbar^2S\sum_i\sum_\delta(a_ia_{i+\delta}^\dagger+a_i^\dagger a_{i+\delta})\left(\sqrt{J^2+D^2}\cos(\delta\theta_{i+\delta}-\delta\theta_i)+J\right)\\
&-\frac{1}{4}\hbar^2S\sum_i\sum_\delta(a_ia_{i+\delta}+a_i^\dagger a_{i+\delta}^\dagger)\left(\sqrt{J^2+D^2}\cos(\delta\theta_{i+\delta}-\delta\theta_i)-J\right)\\
&+\frac{1}{2}K\hbar^2S\sum_i(a_ia_i+a_i^\dagger a_i^\dagger)\sin^2(aqi+\delta\theta_i)
\end{aligned} \tag{A.2.11}$$

Note that our linear part is zero, since it reduces to our set of minimization equations, and these must be satisfied. Since $\delta\theta_i$ is unknown, we can not proceed in simplifying this Hamiltonian any further. Possibly some insight in this deviation $\delta\theta_i$ might help in the diagonalization.

A.3 General identities

In this section we will include the most important identities we used throughout this thesis, each provided with a short description.

The first identity involves some complex exponentials. For the last equality sign we used that we defined a function $\gamma_{\mathbf{k}}$ as $z\gamma_{\mathbf{k}} = \sum_\delta \cos(\mathbf{k}\cdot\delta)$. This equations turns out to be very useful in both the semi-classical and the quantum-mechanical approach.

$$\begin{aligned}
\sum_\delta e^{\pm i\mathbf{k}\cdot\delta} &= \sum_{\delta\in\{a\hat{x},a\hat{y},a\hat{z}\}} e^{\pm i\mathbf{k}\cdot\delta}+e^{\mp i\mathbf{k}\cdot\delta} = 2\sum_{\delta\in\{a\hat{x},a\hat{y},a\hat{z}\}}\cos(\mathbf{k}\cdot\delta)\\
&= \sum_\delta\cos(\mathbf{k}\cdot\delta) = z\gamma_{\mathbf{k}}.
\end{aligned} \tag{A.3.1}$$

Now we get a list of equations for summations involving Fourier transformations for a single operator. One can find the hermitian conjugate of these by using commutation relations for boson operators and conjugating the expression. We also used the previously derived Equation A.3.1. These equalities are written down for an operator a_i, but are exactly the same for an operator b_i.

$$\begin{aligned}
\sum_i\sum_\delta a_i^\dagger a_i &= \frac{1}{z}\sum_{\mathbf{k}} a_{\mathbf{k}}^\dagger a_{\mathbf{k}},\\
\sum_i\sum_\delta a_i^\dagger a_{i+\delta} &= \sum_{\mathbf{k}}\sum_\delta e^{i\mathbf{k}\cdot\delta}a_{\mathbf{k}}^\dagger a_{\mathbf{k}} = z\sum_{\mathbf{k}}\gamma_{\mathbf{k}}a_{\mathbf{k}}^\dagger a_{\mathbf{k}},\\
\sum_i\sum_\delta a_i a_{i+\delta} &= \sum_{\mathbf{k}}\sum_\delta e^{-i\mathbf{k}\cdot\delta}a_{\mathbf{k}}a_{-\mathbf{k}} = z\sum_{\mathbf{k}}\gamma_{\mathbf{k}}a_{\mathbf{k}}a_{-\mathbf{k}}.
\end{aligned} \tag{A.3.2}$$

The next equation is an equation for summations involving Fourier transformations for two operators a_i and b_i. Just as for the previous equation, by using commutation relations, hermitian conjugation, switching a and b, and switching the order of summation according to $\mathbf{k} \to -\mathbf{k}$, all the other necessary equations can be derived.

$$\sum_i \sum_\delta a_i b_{i+\delta} = \sum_{\mathbf{k}} \sum_\delta e^{-i\mathbf{k}\cdot\delta} a_{\mathbf{k}} b_{-\mathbf{k}} = z \sum_{\mathbf{k}} \gamma_{\mathbf{k}} a_{\mathbf{k}} b_{-\mathbf{k}}. \tag{A.3.3}$$

The last equation involves the diagonalization of the Hamiltonian, where we found $\tanh 2\theta_{\mathbf{k}} = -\frac{B_{\mathbf{k}}}{A_{\mathbf{k}}}$ as the condition for these diagonalization. We will provide a short derivation for Method 1 by using identities for hyperbolic trigonometry. The derivation for Method 2 is similar.

$$\begin{aligned} A_{\mathbf{k}}(u_{\mathbf{k}}^2 + v_{\mathbf{k}}^2) + B_{\mathbf{k}} 2u_{\mathbf{k}} v_{\mathbf{k}} = A_{\mathbf{k}} \cosh 2\theta_{\mathbf{k}} + B_{\mathbf{k}} \sinh 2\theta_{\mathbf{k}} &= \frac{A_{\mathbf{k}}}{\sqrt{1 - \frac{B_{\mathbf{k}}^2}{A_{\mathbf{k}}^2}}} - \frac{B_{\mathbf{k}} \frac{B_{\mathbf{k}}}{A_{\mathbf{k}}}}{\sqrt{1 - \frac{B_{\mathbf{k}}^2}{A_{\mathbf{k}}^2}}} \\ &= \frac{1}{A_{\mathbf{k}}} \frac{A_{\mathbf{k}}^2 - B_{\mathbf{k}}^2}{\sqrt{1 - \frac{B_{\mathbf{k}}^2}{A_{\mathbf{k}}^2}}} = \frac{A_{\mathbf{k}}}{|A_{\mathbf{k}}|} \frac{A_{\mathbf{k}}^2 - B_{\mathbf{k}}^2}{\sqrt{A_{\mathbf{k}}^2 - B_{\mathbf{k}}^2}} \\ &= \frac{A_{\mathbf{k}}}{|A_{\mathbf{k}}|} \sqrt{A_{\mathbf{k}}^2 - B_{\mathbf{k}}^2}. \end{aligned} \tag{A.3.4}$$

Note that, in general, we will find that this prefactor is $+1$, but this is something that should be checked. Furthermore, we also used that $A_{\mathbf{k}}$ is typically larger than $B_{\mathbf{k}}$, but this does not need to hold. Note that, in these cases, our frequency becomes complex, which will cause the ground state to become unphysical.

A.4 Numerical results

In this section we will give a comparison between our analytical results on the ground state energy of the antiferromagnetic configuration and the spin-flop configuration, to numerical results. For these numerical results we used an algorithm developed by van Dieten [2015], which is a numerical interpretation of the diagonalization of a quadratic Hamiltonian by Colpa [1978].

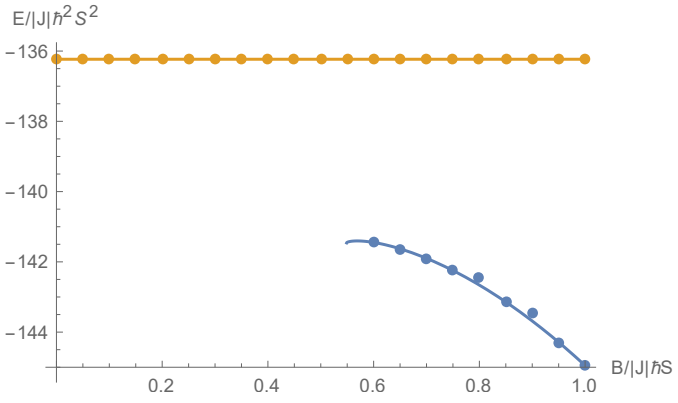

Figure A.1 – Comparison between our analytical computation of the (quantum-mechanical) ground state energies and numerical computations, for both the antiferromagnetic phase and the spin-flop phase. Note that we have set $K/|J| = -0.04$.

Bibliography

F. Bloch. Zur theorie des ferromagnetismus. *Z. Phys.*, 61(3):201–213, 1930.

N.N. Bogoliubov. On a new method in the theory of superconductivity. *Nuovo Cimento*, 7:794, 1958.

J.H.P. Colpa. Diagonalization of the quadratic boson hamiltonian. *Physica A*, 93:327–353, 1978.

I. Dzyaloshinskii. Thermodynamic theory of weak ferromagnetism of antiferromagnetics. *J. Phys. Chem. Solids*, 4:241–255, 1958.

J. Goldstone, A. Salam, and S. Weinberg. Broken symmetries. *Phys. Rev.*, 127(3): 965–970, 1962.

T. Holstein and H. Primakoff. Field dependence of the intrinsic domain magnetization of a ferromagnet. *Phys. Rev.*, 58(12):1098, 1940.

D.I. Khomskii. *Basic Aspects of the Quantum Theory of Solids.* Cambridge University Press, 2010.

S. Mühlbauer, B. Binz, F. Jonietz, C. Pfleiderer, A. Rosch, A. Neubauer, R. Georgii, and P. Böni. Skyrmion lattice in a chiral magnet. *Science*, 323:915–919, 2009.

T. Moriya. Anisotropic superexchange interaction and weak ferromagnetism. *Phys. Rev.*, 120(1):91, 1960.

T.H.R. Skyrme. A unified field theory of mesons and baryons. *Nucl. Phys.*, 31:556–569, 1962.

H.T.C. Stoof, K.B. Gubbels, and D.B.M. Dickerscheid. *Utracold quantum fields.* Springer, 2009.

P. van Dieten. Quantum fluctuations and degeneracies of two-dimensional magnetic skyrmions. Bachelor thesis, Utrecht University, 2015.

S. Schrijnder van Velzen. Quantum fluctuations in antiferromagnetic spin configurations. Bachelor thesis, Utrecht University, 2016.